

Control flow in active inference systems

Chris Fields^{a*}, Filippo Fabrocini^{b,c}, Karl Friston^{d,e}, James F. Glazebrook^{f,g}, Hananel Hazan^a, Michael Levin^{a,h} and Antonino Marcianò^{i,j,k}

^a *Allen Discovery Center at Tufts University, Medford, MA 02155 USA*

^b *College of Design and Innovation, Tongji University, 281 Fuxin Rd, 200092 Shanghai, CHINA*

^c *Institute for Computing Applications “Mario Picone”, Italy National Research Council, Via dei Taurini, 19, 00185 Rome, ITALY*

^d *Wellcome Centre for Human Neuroimaging, University College London, London, WC1N 3AR, UK*

^e *VERSES Research Lab, Los Angeles, CA, 90016 USA*

^f *Department of Mathematics and Computer Science, Eastern Illinois University, Charleston, IL 61920 USA*

^g *Adjunct Faculty, Department of Mathematics,*

University of Illinois at Urbana-Champaign, Urbana, IL 61801 USA

^h *Wyss Institute for Biologically Inspired Engineering at Harvard University, Boston, MA 02115, USA*

ⁱ *Center for Field Theory and Particle Physics & Department of Physics Fudan University, Shanghai, CHINA*

^j *Laboratori Nazionali di Frascati INFN, Frascati (Rome), ITALY*

^k *INFN sezione Roma “Tor Vergata”, I-00133 Rome, ITALY*

March 6, 2023

Abstract

Living systems face both environmental complexity and limited access to free-energy resources. Survival under these conditions requires a control system that can activate, or deploy, available perception and action resources in a context specific way. We show here

*Corresponding author at: Allen Discovery Center at Tufts University, Medford, MA 02155 USA; E-mail address: fieldsres@gmail.com

that when systems are described as executing active inference driven by the free-energy principle (and hence can be considered Bayesian prediction-error minimizers), their control flow systems can always be represented as tensor networks (TNs). We show how TNs as control systems can be implemented within the general framework of quantum topological neural networks, and discuss the implications of these results for modeling biological systems at multiple scales.

Keywords

Bayesian mechanics; Dynamic attractor; Free-energy principle; Quantum reference frame; Scale-free model; Topological quantum field theory

Contents

1	Introduction	3
2	Formal description of the control problem	6
2.1	The attractor picture	6
2.2	The QRF picture	9
2.3	The TQFT picture	14
3	Tensor network representation of control flow	17
3.1	Tensor networks and holographic duality	17
3.2	General results	19
4	Implementing control flow with TQNNs	24
4.1	Tensor networks as classifiers for TQNNs	25
4.2	Geometric RG flow for TQNNs and TNs	26
4.3	TNs as a generalization of the main model architectures in ML	27
5	Implications for biological control systems	29
6	Conclusion	32

1 Introduction

Living things offer remarkable examples of complex, multi-level control policies that guide adaptive function at several scales. At the same time, they are made of components which are usually thought of as physical objects obeying simple rules; how can these two perspectives be unified in a rigorous manner? The framework of *active inference* answers this question by providing a completely general, scale-free formal framework for describing interactions between physical systems in cognitive terms. It is based on the Free Energy Principle (FEP), first introduced in neuroscience [1, 2, 3, 4, 5] before being extended to living systems in general [6, 7, 8, 9] and then to all self-organizing systems [10, 11, 12, 13]. The FEP states that any system that interacts with its environment weakly enough to maintain its identifiability over time 1) has a Markov blanket (MB) that separates its internal states from the states of its environment [14, 15, 16, 17, 18] and 2) behaves over time in a way that asymptotically minimizes a variational free energy (VFE) measured at its MB. Equivalently, the FEP states that any system with a non-equilibrium steady-state (NESS) solution to its density dynamics (and hence an MB) will act so as to maintain its state in the vicinity of its NESS. Any system compliant with the FEP can be described as engaging, at all times, in active inference: a cyclic process in which the system observes its environment, updates its probabilistic “Bayesian beliefs” (i.e., posterior or conditional probability densities) over future behaviors, and acts on its environment so as to test its predictions and gain additional information. The internal dynamics of such a system can be described as inverting a generative model (GM) of its environment that furnishes predictions of the consequences of its actions on its MB.

As a fully-general principle, the FEP applies to all physical systems, not just to behaviorally interesting, plausibly cognitive systems, such as organisms or autonomous robots [10]. Intuitively, behavior is interesting – to external observers and, we can assume, to the behaving system itself – when it is complex, situation-appropriate, and robust in the face of changing environmental conditions. Friston et al. [13] characterize interesting systems as “strange particles”, whose internal (i.e., cognitive) states are influenced by their actions only via perceived environmental responses; such systems have to “ask questions” of their environments in order to get answers [19]. Such systems, even bacteria and other basal organisms [20, 21, 22, 23], have multiple ways of observing and acting upon their environments and deploy these resources in context-sensitive ways. In operations-research language, they exhibit situational awareness, i.e., awareness of the context of actions [24], and deploy attention systems to manage the informational, thermodynamic, and metabolic costs of maintaining such awareness [12, 22]. Situational awareness is dependent on both short- and long-term memory, or more technically, on the period of time over which precise [Bayesian] beliefs exist, sometimes referred to as the temporal depth or horizon of the GM [20, 21]. Upper limits can, therefore, be placed on behavioral complexity by examining the capacity and control of memory systems from the cellular scale [25] upwards. Living systems from microbial mats to human societies employ stigmergic memories [22] and hence have “extended minds” [26] in the sense of the literature on embodied, embedded, enactive, extended, and affective (4EA) cognition [27, 28]. Such memories must be both

readable and writable; hence any system using them must have dedicated, memory-specific perception–action capabilities.

Any system with multiple perception–action (or stimulus–response) capabilities requires a control system that enables context-guided perception and action and precluding the continuous, simultaneous deployment of all available perception–action capabilities. Such self organization entails the selection of a particular course of action – i.e., policy – from all plausible policies entertained by the system’s GM. In the active inference framework, the system’s internal states – hence its GM – can be read as encoding posterior probability densities (i.e., Bayesian beliefs) over the causes of its sensory states, including, crucially, its own actions. This leads to the notion of planning and control as inference [29, 30, 31], with the ensuing selection of an action given by the most likely policy. In bacteria such as *E. coli*, for example, mutual inhibition between gene regulatory networks (GRNs) for different metabolic operons permit the expression of specific carbon-source (e.g., sugar) metabolism pathways only when the target carbon source is detected in the environment [32]. The control of foraging behavior via chemotaxis employs a similar, in this case bistable, mechanism [33]. Such mechanisms are active in multicellular morphogenesis, for example, in the head-versus-tail morphology decision in planaria [34]. In the human brain, mutual inhibition between competing visual processing streams is evident in binocular rivalry (switching between distinct scenes presented to left and right eyes) or in the changing interpretations of ambiguous figures such as the Necker cube [35, 36]; similar competitive effects are observed in other sensory pathways [37]. It also characterizes the competitive interaction between the dorsal and ventral attention systems, which implement top-down and bottom-up targeting of sensory resources, respectively [38]. It is invoked at a still larger scale in global workspace models of conscious processing, in which incoming information streams must compete, with each inhibiting the others, for “access to consciousness” [39, 40]. Mutual inhibition creates an energetic barrier that the control system that implements switching must expend free-energy resources to overcome; the controller must not only turn “on” the preferred system, but also turn “off” the inhibition. The required free energy expenditure in turn induces hysteresis and hence the non-linear, winner-takes-all “switch” behavior in the time regime. Such barriers and their temporal consequences persist in more complex control systems whenever two perception–action capabilities are either functionally incompatible or too expensive to deploy simultaneously.

Switching between perception–action capabilities can be regarded, from a theoretical, FEP perspective, as selecting a plausible policy, or plan, supported by the GM. Technically, the probability distribution over policies or plans can be computed from a free energy functional expected under the posterior predictive density over possible outcomes, as described in §2.1 below. The control system that implements the switching process can be considered to employ the GM to predict, or assign probability distribution to, each perception-action capability (i.e., policy) as a function of context [41, 42]. We can consider the GM to generate probabilistic “beliefs” about the consequences of actions, where here a “belief” is just a mathematically-described structure, e.g., a classical conditional probability density or a quantum state with an assigned amplitude. “Planning” or “control” can, therefore,

always be cast as inference – again in the basal sense of computation – implemented by variational message passing or “belief propagation” on a (normal style) factor graph: a graph with nodes corresponding to the factors of a probability distribution and undirected edges corresponding to message-passing channels. Factor graphs can be combined with message passing schemes, with the messages generally corresponding to sufficient statistics of the factors in question, to provide an efficient computation of functions such as marginal densities [43, 44]. Hence one can formalize control – under the FEP – in terms of control as inference, which implies that there is a description of control in terms of message passing on a factor graph. When the GM is over discrete states, this implies a description of control in terms of tensor operators.

Nearly all simulations of planning – under discrete state space GMs – use the factor-graph formalism. Crucially, the structure of the factor graph embodies the structure of the GM and, effectively, the way that any system represents the (apparent causes of) data on its MB; i.e., the way it “carves nature at its joints,” into states, objects and categorical features. Under the (classical) FEP, the factors that constitute the nodes of the factor graph correspond to the state-space factorization in a mean field approximation, as used by physicists, or by statisticians to implement variational Bayesian (a.k.a., approximate Bayesian) inference [45]. See [46] for technical details, [47] for an application to the brain, and Supplementary Information, Table 1 for a list of selected applications.

We show in this paper that control flow in such systems can always be formally described as a tensor network, a factorization of some overall tensor (i.e., high-dimensional matrix) operator into multiple component tensor operators that are pairwise contracted on shared degrees of freedom [48]. In particular, we show that the factorization conditions that allow the construction of a TN are exactly the same as those that allow the identification of distinct, mutually conditionally independent (in quantum terms, decoherent), sets of data on the MB, and hence allow the identification of distinct “objects” or “features” in the environment. This equivalence allows the topological structures of TNs – many of which have been well-characterized in applications of the TN formalism to other domains [48] – to be employed as a classification of control structures in active inference systems; including cells, organisms, and multi-organism communities. It allows, in particular, a principled approach to the question of whether, and to what extent, a cognitive system can impose a decompositional or mereological (i.e., part-whole) structure on its environment. Such structures naturally invoke a notion of locality, and hence of geometry. The geometry of spacetime itself has been described as a particular TN – a multiscale entanglement renormalization ansatz (MERA) [49, 50, 51] – suggesting a deep link between control flow in systems capable of observing spacetime (i.e., capable of implementing internal representations of spacetime) and the deep structure of spacetime as a physical construct.

We begin in §2 by analyzing the control-flow problem in three different representations of active inference. First, we employ the classical, statistical formulation of the FEP [10, 11] in §2.1 to describe control flow as implementing discrete, probabilistic transitions between dynamical attractors on a manifold of computational states. We then reformulate the physical interaction in quantum information-theoretic terms in §2.2; in this formulation [12],

components of the GM can be considered to be distinct quantum reference frames (QRFs) [52, 53] and represented by hierarchical networks of Barwise-Seligman classifiers [54] as developed in [55, 56, 57, 58]. Control flow then implements discrete transitions between QRFs. The third step, in §2.3, employs the mapping between hierarchies of classifiers and topological quantum field theories (TQFTs) developed in [59]. Here, control flow is implemented by a TQFT, with transition amplitudes given by a path integral. The second and third of these representations provide formal characterizations of intrinsic (or “quantum”) context effects that are consistent with both the sheaf-theoretic treatment of contextuality in [60, 61] and the Contextuality by Default (CbD) approach of [62, 63]; see also the discussion in [57] and [59, §7.2]. The underlying theme is that contextuality arises due to the non-existence of any globally definable (maximally connected) conditional probability distribution across all possible observations (see e.g., [64] for a review from a more general physics perspective). Extending our earlier analysis [57], we discuss reasons to expect that active inference systems will generically exhibit such context effects.

We then develop in §3 a fully-general tensor representation of control flow, and prove that this tensor can be factored into a TN if, and only if, the separability (or conditional statistical independence) conditions needed to identify distinct features of or objects in the environment are met. We show how TN architecture allows classification of control flows, and give two illustrative examples. We discuss in §4 several established relationships between TNs and artificial neural network (ANN) architectures, and how these generalize to topological quantum neural networks [59, 65], of which standard deep-learning (DL) architectures are a classical limit [66]. We turn in §5 to implications of these results for biology, and discuss how TN architectures correlate with the observational capabilities of the system being modeled, particularly as regards abilities to detect spatial locality and mereology. We consider how to classify known control pathways in terms of TN architecture and how to employ the TN representation of control flow in experimental design. We conclude by looking forward to how these FEP-based tools can further integrate the physical and life sciences.

2 Formal description of the control problem

2.1 The attractor picture

Let U be a random dynamical system that can be decomposed into subsystems with states $\mu(t)$, $b(t)$, and $\eta(t)$ such that the dependence of the $\mu(t)$ on the $\eta(t)$, and vice-versa, is only via the $b(t)$. In this case, the $b(t)$ form an MB separating the $\mu(t)$ from the $\eta(t)$. We will refer to the $\mu(t)$ as “internal” states, to the $\eta(t)$ as “environment” states, and to the combined $\pi(t) = (b(t), \mu(t))$ as “particular” (or “particle”) states [10]. The FEP is a variational or least-action principle stating that any system – that interacts sufficiently weakly with its environment – can be considered to be enclosed by an MB, i.e. any “particle” with states $\pi(t) = (b(t), \mu(t))$, will evolve in a way that tends to minimize a variational free energy

(VFE) $F(\pi)$ that is an upper bound on (Bayesian) surprisal. This free energy is effectively the divergence between the variational density encoded by internal states and the density over external states conditioned on the MB states. It can be written [10, Eq. 2.3],

$$\begin{aligned}
F(\pi) &= \underbrace{\mathbb{E}_{q(\eta)}[\ln q_\mu(\eta) - \ln p(\eta, b)]}_{\text{Variational free energy}} \\
&= \underbrace{\mathbb{E}_q[-\ln p(b|\eta) - \ln p(\eta)]}_{\text{Energy constraint (likelihood \& prior)}} - \underbrace{\mathbb{E}_q[-\ln q_\mu(\eta)]}_{\text{Entropy}} \\
&= \underbrace{D_{KL}[q_\mu(\eta)||p(\eta)]}_{\text{Complexity}} - \underbrace{\mathbb{E}_q[\ln p(b|\eta)]}_{\text{Accuracy}} \\
&= \underbrace{D_{KL}[q_\mu(\eta)||p(\eta|b)]}_{\text{Divergence}} - \underbrace{\ln p(b)}_{\text{Log evidence}} \geq -\ln p(b)
\end{aligned} \tag{1}$$

The VFE functional $F(\pi)$ is an upper bound on surprisal (a.k.a. self-information) $\mathfrak{I}(\pi) = -\ln p(\pi) > -\ln p(b)$ because the Kullback-Leibler divergence term (D_{KL}) is always non-negative. This KL divergence is between the density over external states η , given the MB state b , and a variational density $Q_\mu(\eta)$ over external states parameterized by the internal state μ . If we view the internal state μ as encoding a posterior over the external state η , minimizing VFE is, effectively, minimizing a prediction error, under a GM encoded by the NESS density. In this treatment, the NESS density becomes a probabilistic specification of the relationship between external or environmental states and particular (i.e., “self”) states. We can interpret the internal and active MB states in terms of active inference, i.e., a Bayesian mechanics [11], in which their expected flow can be read as perception and action, respectively. Here “active” states are a subset of the MB states that are not influenced by environmental states and – for the kinds of particles considered here – do not influence internal states. In other words, active inference is a process of Bayesian belief updating that incorporates active exploration of the environment. It is one way of interpreting a generalized synchrony between two random dynamical systems that are coupled via an MB.

If the “particle” π is a biological cell, it is natural to consider the MB b to be implemented by the cell membrane and the “internal” states μ to be the internal macromolecular or biochemical states of the cell; indeed, it is this association that motivated the application of the FEP to cellular life [5]. In this case, the NESS corresponds to the state, or neighborhood of states, that maintain homeostasis (or more broadly, allostasis [67, 68, 69]) and hence maintain the structural and functional integrity of π as a living cell. This activity of self-maintenance has been termed “self-evidencing” [70]; systems compliant with the FEP can be considered to be continually generating evidence of – or for – their continued existence [10].

In the terminology of [13] cells are “strange particles” – their signal transduction pathways monitor (components of) the states of their environments, but do not directly monitor their actions on their environments (i.e., their own active states). The consequences of any action

can only, therefore, be deduced from the response of the environment. In this situation, causation is always uncertain: whether an action by the environment on the cell – what the cell detects as an environmental state change – is a causal consequence of an action the cell has taken in the past cannot be determined by the data available to the cell. Every action, therefore, increases VFE, while every observation (potentially) decreases it. The (apparent) task of the cell’s GM is to minimize the increases, on average, while maximizing the decreases.

The Bayesian mechanics afforded by the FEP implies a (classical) thermodynamics; indeed, the FEP can be read as a constrained maximum entropy or caliber principle [71, 72] (Sakthivadivel 2022, Sakthivadivel 2022). This follows from the fact that inference, i.e., self evidencing, entails belief updating and belief updating incurs a thermodynamic cost via the Jarzynski equality [73, 74, 75]. This cost provides a lower bound on the thermodynamic free energy required for metabolic maintenance. For example, a cell’s actions on its environment – e.g., chemotactic locomotion – are largely driven by the need to acquire thermodynamic free energy. The cell’s GM cannot, therefore, minimize VFE by minimizing action [76]; instead, it must successfully predict which actions will replenish its free-energy supply. As actions are energetically expensive, this requires trading off short-term costs against long-term goals. As shown in [41], selective pressures operating on different timescales favor the development of metaprocessors that control lower-level actions in a context-dependent way; these are often implemented via a hierarchical GM [77]. Such meta-level control provides probabilistic models of risk-sensitive actions in context.

While such systems may be described as regulating free-energy seeking actions, they also regulate information-seeking actions, i.e., curiosity-driven exploration [78, 79, 80]. This follows because VFE provides an upper bound on complexity minus accuracy [81]. The expected free energy (EFE), conditioned upon any action, can therefore be scored in terms of expected complexity and expected inaccuracy. Expected complexity is “risk” and corresponds to the degree of belief updating that incurs a thermodynamic cost; leading to risk-sensitive control (e.g., phototropism). Expected inaccuracy corresponds to “ambiguity” leading to epistemic behaviors (e.g., searching for lost keys under a streetlamp) [42].

When context-dependent control is considered, the neighborhood of the NESS resolves into a network of local minima corresponding to fixed perception-action loops separated by energetic barriers that the control system must overcome to switch between loops. For example, in a cell, this energetic barrier comprises the energy required to activate one pathway while de-activating another, which may include the energetic costs of phosphorylation, other chemical modifications, additional gene expression, etc. Different pairs of pathways can be expected to be separated by energetic barriers of different heights, generating a topographically-complex free energy landscape that coarse-grains, in a long-time average, to the neighborhood of the NESS, i.e., to the maintenance of allostasis [68, 69, 82].

As noted earlier, we can think of controllable perception-action loops as nodes on a factor graph, with the edges corresponding to pathways for control flow, and the transition probabilities labeling the edges as inversely proportional to the energetic barrier between loops. This allows representing the GM for meta-level control (i.e., hierarchical) as a message-

passing system as described in [47]. The presence of very high energetic barriers can render such a GM effectively one-way, as seen in the context-dependent switches between signal transduction pathways and GRNs that characterize cellular differentiation during morphogenesis. Biological examples of these include modifications of bioelectric pattern memories in planaria, which can create alternative-species head shapes that eventually remodel back to normal [83], or produce 2-headed worms which are permanent, and regenerate as 2-headed in perpetuity [84].

2.2 The QRF picture

Cellular information processing has traditionally been treated as completely classical, i.e., as implemented by causal networks of macromolecules, each of which undergoes classical state transitions via local dynamical processes that are conditionally independent of the states of other parts of the network. While the “quantum” nature of proteins and other macromolecules is broadly acknowledged, the scale at which quantum effects are important remains controversial, with straightforward single-molecule decoherence models predicting decoherence times of attoseconds (10^{-18} s) or less [85, 86]: several orders of magnitude below the timescales of processes involved in molecular information processing [87]. While functional roles for quantum coherence in intramolecular information processing have been demonstrated, intermolecular coherence remains experimentally elusive [88, 89, 90, 91].

The free-energy budgets of both prokaryotic and eukaryotic cells are, however, orders of magnitude smaller than would be required to support fully-classical information processing at the molecular scale, suggesting that cells employ quantum coherence as a computational resource [92]. Indirect evidence of longer-range, tissue-scale coherence in brains has also been reported [93]. Reformulating the FEP in quantum information-theoretic terms enables it to describe situations in which long-range coherence, and hence quantum computation, cannot be neglected.

Following the development in [12], we consider a bipartite decomposition $U = AB$ of a finite, isolated system U for which the interaction Hamiltonian $H_{AB} = H_U - (H_A + H_B)$ is sufficiently weak over the time period of interest that the joint state U is separable (i.e., factors) as $|U\rangle = |A\rangle|B\rangle$. In this case, we can choose orthogonal basis vectors $|i^k\rangle$ so that:

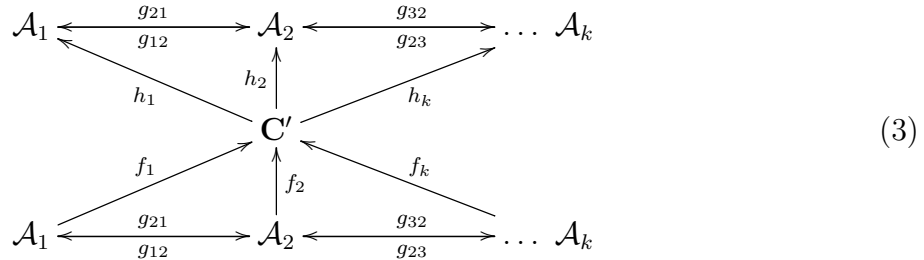
$$H_{AB} = \beta_k K_B T_k \sum_i^N \alpha_i^k M_i^k, \quad (2)$$

where K_B denotes Boltzmann’s constant, T is the absolute temperature of the environment, $k = A$ or B , the M_i^k are N mutually-orthogonal Hermitian operators with eigenvalues in $\{-1, 1\}$, the $\alpha_i^k \in [0, 1]$ are such that $\sum_i^N \alpha_i^k = 1$, and $\beta_k \geq \ln 2$ is an inverse measure of k ’s thermodynamic efficiency that depends on the internal dynamics H_k ; see [56, 58, 94, 95] for further motivation and details of this construction and [96] for a pedagogical review. This description is purely topological, attributing no geometry to either U or \mathcal{B} ; hence it allows

the “embedding space” of perceived “objects” to be an observer-dependent construct. It has several relevant consequences:

- We can regard A and B as separated, and determined by independent measures. They are separated by – and interact via – a holographic screen \mathcal{B} that can be represented, without loss of generality, by an array of N non-interacting qubits, where N is the dimension of H_{AB} [94, 95].
- A and B can be regarded as exchanging finite N -bit strings, each of which encodes one eigenvalue of H_{AB} [94].
- A and B have free choice of basis for H_{AB} , corresponding to free choice of local frames at \mathcal{B} , e.g., free choice, for each qubit q_i on \mathcal{B} , of the local z axis and hence the z -spin operator s_z that acts on q_i [96].
- Choice of basis corresponds to choosing the zero-point of total energy) by each of A and B . The systems A and B are, therefore, in general at informational, but not at thermal equilibrium [12].
- As A and B must obtain from B or A , respectively, whatever thermodynamic free energy is required, by Landauer’s principle [73, 99, 100], to fund the encoding of classical bits on \mathcal{B} (as well as any other irreversible classical computation), A and B must each devote some sector F of \mathcal{B} to free-energy acquisition. The bits in F are “burned as fuel” and so do not contribute input data to computations. Waste-heat dissipation by one system is free energy acquisition by the other. The free-energy sectors F_A and F_B of A and B need not align as subsets of qubits on \mathcal{B} ; that is, qubits that A regards as free-energy sources may be regarded by B as informative outputs and vice-versa [56, 58].
- The actions of the internal dynamics H_A and H_B on \mathcal{B} can be represented by A - and B -specific sets of QRFs, each of which both “measures” and “prepares” qubits on \mathcal{B} . Each QRF acts on the qubits in some specific sector of \mathcal{B} , breaking the permutation symmetry of Eq. (2) [56, 58, 59]. Only QRFs acting on sectors other than F implement informative computations; we will therefore restrict attention to these QRFs.
- Each “computational” QRF can, without loss of generality, be represented by a cone-cocone diagram (CCCD) comprising Barwise-Seligman classifiers and infomorphisms between them [54, 55]. The apex of each such CCCD is, by definition, both the category-theoretic limit and colimit of the “input/output” classifiers that correspond, formally, to the operators M_i^k in Eq. (2) [56, 58, 59].

Typically, a CCCD is structured as a distributed information flow in the form:



incorporating sets of classifiers $\{A_\alpha\}$ and (logic) infomorphisms $\{f_i, g_{jk}\}$ [54, Ch 12] over suitable index ranges. As a memory-write system, Diagram (3) depicts a generic a blueprint for a bow-tie or variational autoencoder (VAE) network amenable to describing a hierarchical Bayesian network with belief-updating as discussed in e.g. [12, 57, 59]. Crucially, it is the non-commutativity of CCCDs of this form that specifies intrinsic or quantum contextuality, as occurs, for instance, when the colimit core \mathbf{C}' is undefinable [57, §7, §8] [59, §7.2]. Consequences of such contextuality are discussed via examples in §5.

The holographic screen \mathcal{B} functions as an MB separating A from B . It can be regarded as having an N -dimensional, N -qubit Hilbert space $\mathcal{H}_{q_i} = \prod_i q_i$. While \mathcal{H}_{q_i} is strictly ancillary to $\mathcal{H}_U = \mathcal{H}_A \otimes \mathcal{H}_B$, the classical situation can be recovered in the limit in which the entanglement entropies $\mathcal{S}(|A\rangle), \mathcal{S}(|B\rangle) \rightarrow 0$ by considering the products $\mathcal{H}_A \otimes \mathcal{H}_{q_i}$ and $\mathcal{H}_B \otimes \mathcal{H}_{q_i}$ to be “particle” state spaces for A and B , respectively. In this classical limit, the states of \mathcal{H}_{q_i} become the blanket states of an MB that functions as a classical information channel [94, 95, 96]. In quantum holographic coding, for example, \mathcal{B} is often represented by a polygonal tessellation of the hyperbolic disc, with qubits represented by polygonal centroids. A specific TN model of a pentagon code is developed in [97]; see in particular their Fig. 4. The geometric description of \mathcal{B} as implementing holographic coding, and its classical limit as an MB structured as a direct acyclic graph (DAG), is further explored in the setting of TQNNs in [98].

In this quantum-theoretic picture, “systems” or “objects” observed and manipulated by A or B correspond to sectors on \mathcal{B} that are the domains of particular QRFs deployed by A or B , respectively [58, 12, 59]. To simplify notation, we use the same symbol, e.g., ‘ Q ’ to denote both a QRF Q and the sector $\text{dom}(Q)$ on \mathcal{B} . Any identifiable system X factors into a “reference” component R that maintains a time-invariant state $|R\rangle$ or more generally, state density ρ_R , that allows re-identification and hence sequential measurements over extended time, and a “pointer” component P with a time-varying state $|P\rangle$ or density ρ_P . It is this pointer component, named for the pointer of an analog instrument, which is the “state of interest” for measurements. The QRFs R and P clearly must commute, and the sectors R and P clearly must be mutually decoherent [58, 12, 59]. All “system” sectors must be components of some overall sector E that corresponds to the “observable environment.” The recording of measurement outcomes to a classical memory and the reading of previously-recorded outcomes from memory can similarly be represented by a QRF Y . As $\text{dom}(Y)$ is a sector on \mathcal{B} , recorded memories of A are exposed to and hence

subject to modification by B and vice-versa. Both the observable environment E and the memory sector Y must be disjoint from, and decoherent with, the free-energy sector F .

As actions on \mathcal{B} encode classical data, they have an associated free energy cost of at least $\ln 2 K_B T$ per bit [73, 99, 100] that must originate from the source at F . Time-energy complementary associates a minimum time of $h/[\ln 2(K_B T)]$, with h being the Planck's constant, to this energy expenditure. We can, therefore, associate actions on \mathcal{B} , including memory writes, with “ticks” of an internal time QRF, which we denote t_A and t_B for A and B , respectively. Assuming all observational outcomes are written to memory, we can represent the situation as in Fig. 1. The time QRF is effectively an outgoing bit counter that can be represented by a groupoid operator $\mathcal{G}_{ij} : t_i \rightarrow t_j$ [56]. As outgoing bits are oriented in opposite directions with respect to \mathcal{B} for A and B , the time “arrows” t_A and t_B point in opposite directions. Hence A and B can both be regarded as “interacting with their own futures” as discussed in [96].

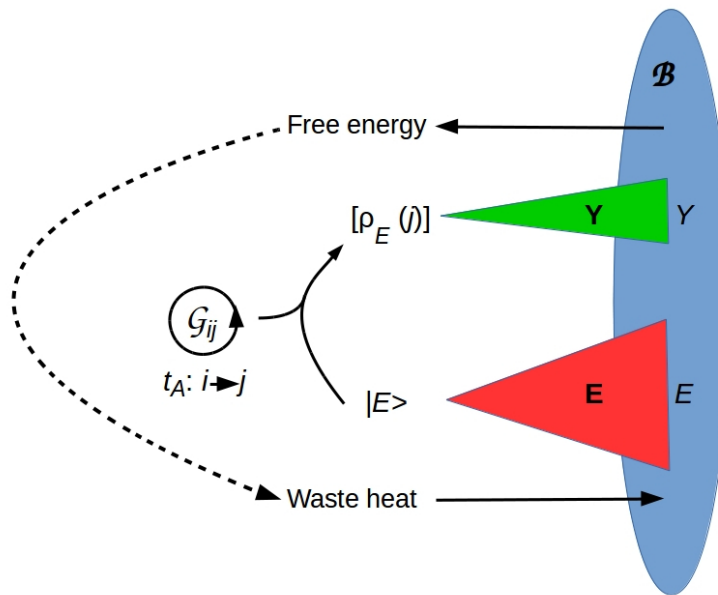
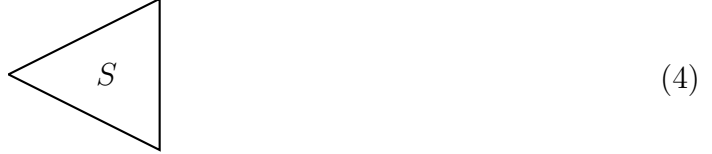


Figure 1: Cartoon illustration of QRFs required to observe and write a readable memory of an environmental state $|E\rangle$. The QRFs \mathbf{E} and \mathbf{Y} read the state from E and write it to the memory Y respectively. Any identified system S must be part of E . The clock \mathcal{G}_{ij} is a time QRF that defines the time coordinate t_A . The dashed arrow indicates the observer's thermodynamic process that converts free energy obtained from the unobserved sector F of \mathcal{B} to waste heat exhausted through F . Adapted from [58], CC-BY license.

Measurements of a system X can be considered sequential if: 1) they separated in time according to the internal time QRF, and 2) their outcomes are recorded to memory to enable comparability across time. We show in [59] that sequential measurements can always be

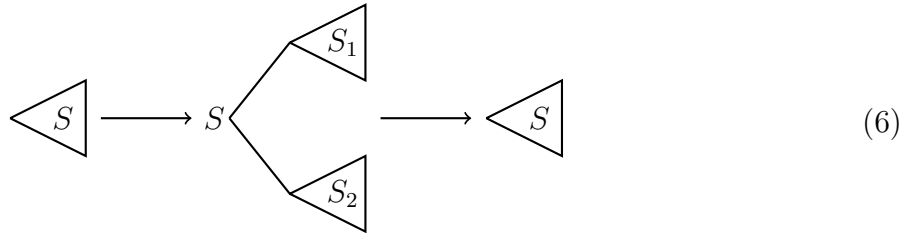
represented by one of two schemata. Using the compact notation:



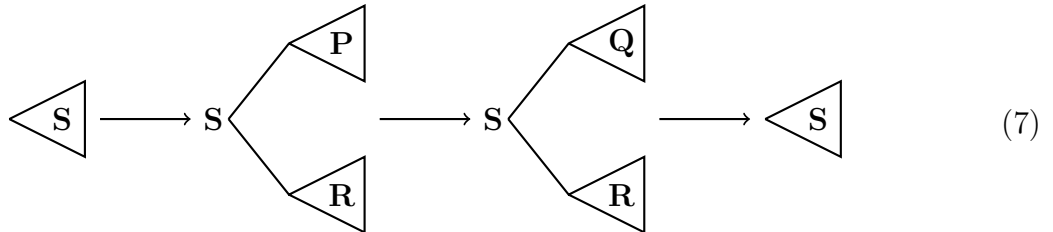
to represent a QRF S , we can represent measurements of a physical situation in which one system divides into two, possibly entangled, systems with a diagram of the form:



Parametric down-conversion of a photon exemplifies this kind of process. The reverse process can be added to yield:



In the second type of sequential measurement process, the pointer-state QRF P is replaced with an alternative QRF Q with which it does not commute. Sequences in which position and momentum, s_z and s_x are measured alternately are examples. These can be represented by the diagram



As both P and Q must commute with R , the commutativity requirements for S are satisfied. The sequences of operations depicted in Diagrams (6) and (7) clearly raise the questions of how control is implemented, and of how the context changes that drive control flow are detected. Before turning to these questions in §3, we review a path-integral representation of QRFs, show that the same representation captures the behavior of any system X identified by a QRF, and discuss the questions of multiple observers and quantum contextuality.

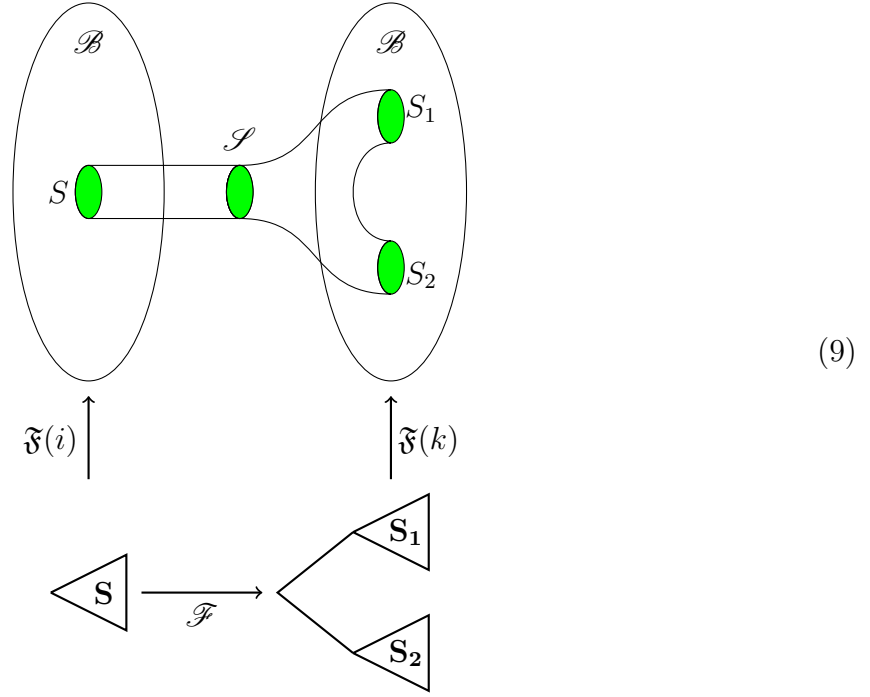
2.3 The TQFT picture

As a least-action principle, the FEP is fundamentally a statement about the paths followed by the joint system U through its state space. The classical FEP is amenable to a path-integral formulation [13] that expresses the expected value of any observable (functional) $\Omega[x(t)]$ of paths $x(t)$ through the relevant state space as ([101], Eq. 6):

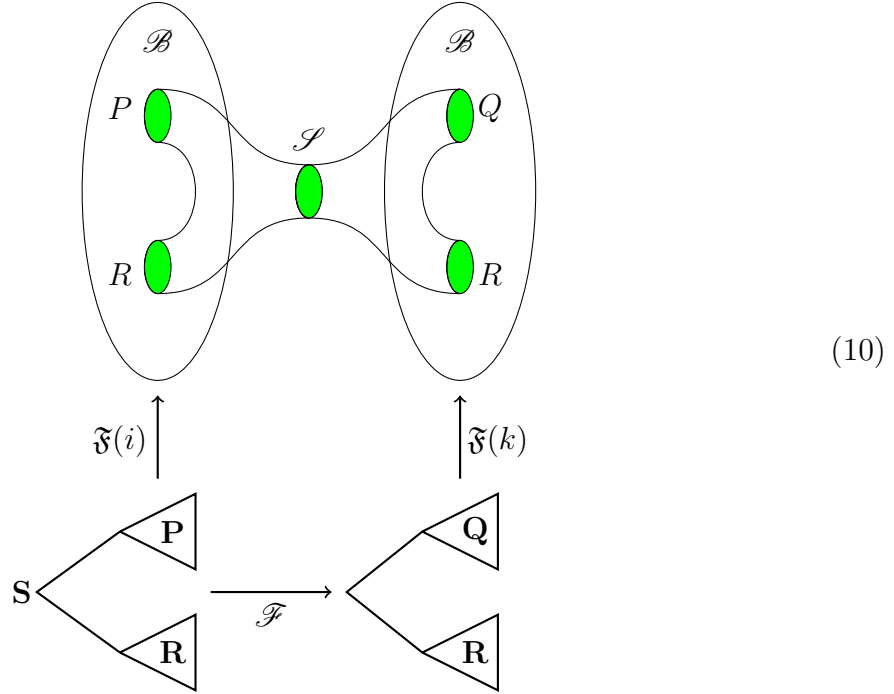
$$\langle \Omega[x(t)] \rangle = \int dx_0 \int d[x(t)] \Omega[x(t)] p(x(t)|x_0) p_0(x_0) \quad (8)$$

where x_0 is the initial state and $p(x(t)|x_0)$ is the conditional probability of the path $x(t)$. Quantum theory generalizes this expression by, effectively, replacing $\Omega[x(t)]$ with an automorphism on the relevant Hilbert space and $p(x(t)|x_0)$ with an amplitude for $x(t)$ given the initial state x_0 . For some finite-dimensional Hilbert space \mathcal{H} , the manifold of all such automorphisms is a cobordism on \mathcal{H} , which is by definition a TQFT on \mathcal{H} [102].

We show in [59] that any sequential measurement of any sector X of \mathcal{B} induces a TQFT on X , considered as a projection of the N -dimensional boundary Hilbert space \mathcal{H}_{q_i} associated with \mathcal{B} . In particular, measurement sequences of the form of Diagram (6) can be mapped to cobordisms, i.e., to manifolds of maps between two designated boundaries, of the form:



while sequences of the form of Diagram (7) can be mapped to cobordisms of the form:



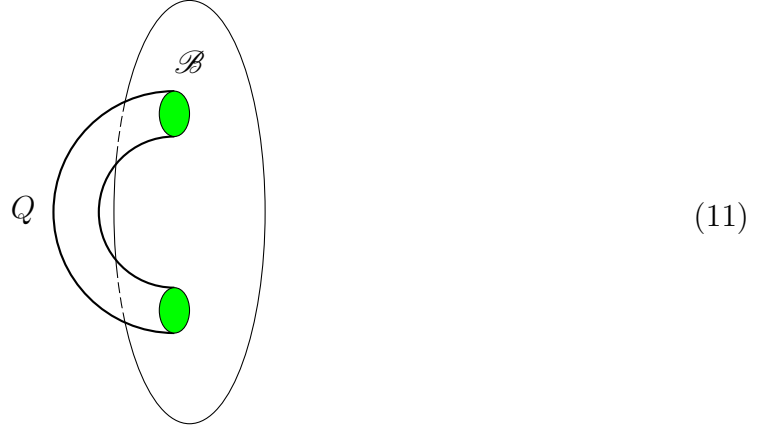
In either case, $\mathfrak{F} : \mathbf{CCCD} \rightarrow \mathbf{Cob}$ is the functor from the category **CCCD** of CCCDs (and hence of QRFs) to the category of **Cob** finite cobordisms required to define a TQFT. In general, we can state:

Theorem 1 ([59] Thm. 1). *For any morphism \mathcal{F} of CCCDs in **CCCD**, there is a cobordism \mathcal{S} such that a diagram of the form of Diagram (9) or (10) commutes.*

referring to [59] for the proof.

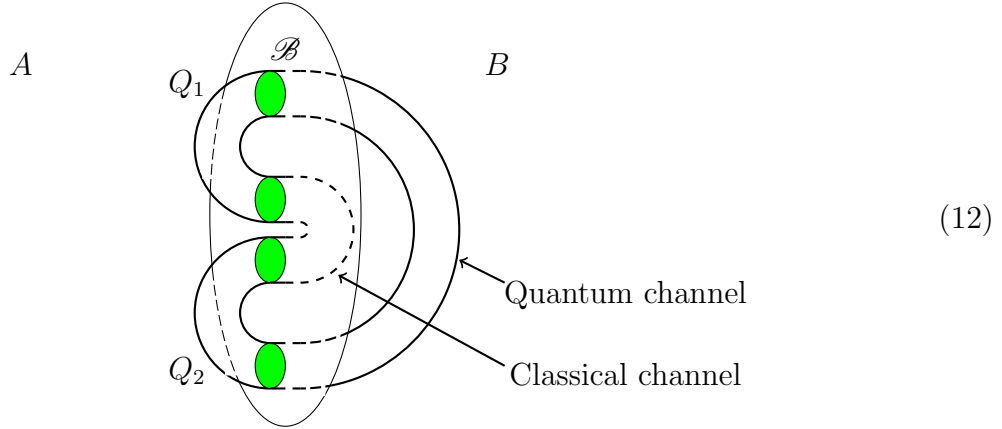
Theorem 1 applies to any sequential measurement; therefore, it applies to measurements of a sector X followed by measurements of the associated memory sector Y , or vice versa. Assuming for convenience $\dim(X) = \dim(Y)$, we can consider a composite operation $Q = (\overrightarrow{Q}, \overleftarrow{Q})$, where $\overrightarrow{Q} = Q_X Q_Y$ and $\overleftarrow{Q} = Q_Y Q_X$, is then a pair of QRF sequences that can be identified with TQFTs that measure and record an outcome, mapping $\mathcal{H}_X \rightarrow \mathcal{H}_Y$, and dually use an outcome read from memory to prepare a state, mapping $\mathcal{H}_Y \rightarrow \mathcal{H}_X$,

respectively as in Diagram 11:



This composite operator Q is, by Theorem 1, a TQFT [98]. Hence the operation of recording observational outcomes for a sector X made at t to memory, and then comparing them to later observations at $t + \Delta t$, is formally equivalent to propagating the “system” X forward in time from t to $t + \Delta t$.

Identifying QRFs as “internal” TQFTs allows a general analysis of information exchange between multiple QRFs deployed by a single system, e.g., A . Because all QRFs act on \mathcal{B} , information exchange between QRFs requires a channel that traverses B . Any such channel is itself a QRF, one deployed by B . Considering A to comprise two observers, one deploying Q_1 and the other deploying Q_2 , that interact via a local operations, classical communication (LOCC [103]) protocol provides an example:



In a LOCC protocol, one channel is considered “classical” while the other is considered “quantum”; however, this language masks the fact that both channels are physical. As pointed out in [104], all media supporting classical communication are physical, and interactions with these media are always local measurements or preparations. Hence the two channels in a LOCC protocol are physically equivalent – both are TQFTs implemented by B – although their conventional semantics are different.

Diagram (12) can, clearly also represent externally-mediated communication between any two functional components of a system, e.g., macromolecular pathways within a cell or functional networks within a brain. We show in [98] that whenever Q_1 and Q_2 are deployed by distinct – technically, separable or mutually decoherent – “observers” or “systems,” they fail to commute, i.e., the commutator $[Q_1, Q_2] = Q_1 Q_2 - Q_2 Q_1 \geq h/2$, where again h is Planck’s constant. As shown in [57], Theorem 3.4 using the CCCD representation, non-commutativity of QRFs induces quantum contextuality, i.e., dependence of measurement results on “non-local hidden variables” that characterize the measurement context [105, 106, 107]. In the current context, such hidden variables characterize the action of H_B on \mathcal{B} , affecting what A will observe next in every cycle of A - B interaction.

As shown in [63], such context dependence can, in principle, be captured classically if sufficient measurements of the context can be implemented. Such measurements would, however, have to access all of B . The existence of an MB prevents such access; in the current setting, A has access to B only via \mathcal{B} . The finite energetic cost of measurement, and consequent requirement for a thermodynamic sector F , prevents measurement even of all of \mathcal{B} by any finite physical system. Hence, we can expect physical systems, including all biological systems, to employ only local context-dependent control to switch between mutually non-commuting (sets of) QRFs. How context switches implemented by QRF switches induce evolution, development and learning was introduced in [22]. Some specific of context switching will be discussed §5.

3 Tensor network representation of control flow

3.1 Tensor networks and holographic duality

Entanglement and quantum error correction, two concepts developed in quantum information theory, have been proved to have a fundamental role in unveiling quantum gravity [108]. At the origin of this consideration there has been the discovery by Bekenstein and Hawking [109, 110, 111, 112] that the second law of thermodynamics can be preserved in the gravitational field of a black hole, if this latter has an entropy proportional to the area of its horizon, by the inverse of the Newton gravitational constant G . This entropy is maximal, as implied by the second law itself, providing an upper bound for possible configurations of matter within a region of the same size [113, 114].

Nonetheless, the scaling of the local degrees of freedom counted by the entropy does not increase as the volume, hinging toward the formulation of the holographic conjecture [115], suggesting a division between the information that can only be retrieved on the boundary world, and a merely apparent bulk world. AdS/CFT realized the holographic conjecture, postulating a duality between gravity in asymptotically AdS space and quantum field theory on the spatial infinity of the AdS space [116]. Giving literal meaning to the duality, Ryu and Takayanagi (RT) proposed that entanglement of a boundary region fulfils the same law

as for the black hole entropy, replacing the area of the black hole horizon with an extremal surface area that bounds the bulk region under scrutiny.

While on the boundaries the theory can be individuated assigning a specific conformal field theory (CFT), in the bulk the geometry can be associated to specific entanglement structures of the quantum systems. This is for instance what happens to the ground states of a CFT associated to an AdS space: the RT area surface increases less fast than the volume of the boundary. When the boundary is at equilibrium, in a thermal state of finite temperature, the bulk geometry corresponds to that of a black hole, its horizon being parallel to the boundary and its size increasing with the temperature. The RT surface is then confined between the boundary and the back hole horizon, approaching the boundary at higher temperature and increasing its entropy. These considerations suggest the existence of a subtle link interconnecting the structure of space-time and quantum entanglement, and hence that a theory of quantum gravity must be fundamentally holographic, where its states satisfy the RT formula for some bulk geometry.

The existence of an exact correspondence between bulk gravity and quantum theory at the boundary may hinge toward possible inconsistencies with locality. This has been discussed in the literature, in terms of local reconstruction theory [117, 118, 119]: variables in the bulk (e.g. bulk spins) can be controlled instantaneously from the boundary, but requiring simultaneous access to a large portion of the boundary: locality and upper speed of light do not hold exactly in this theory. Nonetheless, local observers confined in small regions at the boundary still fulfil locality and the existence of an upper limit of the speed of information exchange, in a way that is reminiscent of quantum error correction code (QECC) in quantum information theory: information is stored redundantly, in such a way that when part of it is corrupted, a reconstruction of information is still possible. Locality in the bulk is therefore a QECC property of the encoding map that realizes the duality between bulk and boundary. On the other hand, these properties are strictly connected to RT, which provides the necessary resource of entanglement for QEEC to emerge.

The RT formula and QECC are properties fulfilled by different classes of models, among which TNs [120]. These have been first introduced in condensed matter physics as variational wave-functions of strongly correlated systems [121, 122]. TNs are many-body wave-functions that can be derived composing few-body quantum states, which are indeed tensors. A prototype of TN is e.g. the Einstein-Podolsky-Rosen (EPR) entangled pairs of qubits: in an entangled basis, measured qubits are in some entangled pure state and can be composed with remaining ones with increasing complexity: complicated quantum entanglement can be derived by only entangling a few qubits [123].

Particularly relevant for its implications on the reconstruction of the space-time structure is the multi-scale entanglement renormalization ansatz (MERA) [124]. TNs can be naturally related to holography duality by considering that their entanglement entropy can be controlled by their graph geometry. Some versions of TNs that are characterized by RT entanglement entropy and QEEC have been constructed resorting to stabilizer codes [125, 126] and random tensors with large bond dimension [127]. TNs with random tensors at each node can be regarded as random states restricted by the topology of the network.

Exactly as random states are almost maximally entangled, random TNs show through the RT formula an almost maximal entanglement, providing a large family of states with interesting properties to explore holographic duality. Furthermore, for random TNs the RT formula holds in generic spaces with not necessarily hyperbolic geometry, hinging toward an extension of holographic duality beyond AdS, to more general configurations in quantum gravity. Nonetheless, at least in three dimensions, random tensor networks have been related to the gravitational action, by means of the Regge calculus [128].

On the other hand, since geometry emerges as a specification of the entanglement structure, one may consider that the Einstein equations should be connected as well to the dynamics of entanglement. For small perturbations around the ground state of a CFT in boundary, linearized Einstein equations have been derived from the RT formula [129, 130]. Indeed, the conformal symmetry enables a relations between the energy momentum and the entanglement entropy, and consequently the area of the extremal surface c can be connected to the energy-momentum distribution at the boundary — this is equivalent to the linearized Einstein equations.

The dynamics on the boundary, on the other side, shows a chaotic behaviour, with scrambling of the single-particle operators, which evolve into multi-particle operators [131]. Maximal chaotic behaviour recovered in the ladder operators commutator growth, is encoded in the out-of-time-ordered correlation (OTOC) functions, characterized by exponential growth in time and temperature. A model endowed with this properties is e.g. the Sachdev-Ye-Kitaev model, developed to describe certain systems in condensed matter physics, such as Gapless spin-fluid [132, 133, 134]. On the other hand, operator scrambling is also related to QECC: the chaotic dynamics at the boundary instantiates QECC preserving quantum information, efficiently hidden (and protected) behind the horizon. Nevertheless this has led to many questions, concerning the information behind the horizon being eventually accessible from the boundary though non-local measurements, the fate of the local degrees of freedom hitting the singularity, the relation among the causal structure of the bulk and a smooth geometry across the horizon.

3.2 General results

We can move to prove a general result:

Theorem 2. *A system A exhibits non-trivial control flow if, and only if, its control flow can be represented by a TN.*

and examine some of its corollaries. We begin by defining:

Definition 1. *Control flow is trivial if a system deploys only one QRF.*

As any collection of mutually-commuting QRFs can be represented as a single QRF [57, 59], any system that deploys only mutually-commuting QRFs exhibits trivial control flow.

Systems that deploy only a single QRF “do the same thing” regardless of context, and so do not qualify as “interesting” in the sense used here. As noted above, no finite physical system can measure the entire state of its boundary with a single QRF, so no such system can simultaneously measure and act on its entire context. Any system A that deploys multiple QRFs in sequence cannot, as noted above, avoid contextuality due to unobservable effects, mediated by the action of H_B , of the action of Q_i on the state measured by Q_j . Every action taken by an “interesting” system, in other words, at least transiently increases the VFE at its boundary.

Consider, then, a system A that deploys multiple, distinct QRFs Q_1, Q_2, \dots, Q_n , where $n \ll N = \dim(H_{AB})$. Classical control flow in A can then be represented by a matrix $\mathbf{CF} = [P_{ij}]$, where P_{ij} is the probability of the control transition $Q_i \rightarrow Q_j$. As noted earlier, any such transition has an energetic cost, which must be paid with free energy sources from F .

The matrix \mathbf{CF} is a 2-tensor. Theorem 2 states that this tensor can be decomposed into a TN. We prove it as follows:

Proof (Thm. 2). Suppose first that control flow in a system A can be represented by a TN. A TN is, by definition, a factorization of a tensor operator into a network of tensor operators. This network can be either hierarchical or flat; if it is hierarchical, each layer can be considered a flat TN. Hence no generality is lost in considering just the case of a flat TN, which is an operator contraction $T = \dots T_{ij} T_{jk} T_{kl} \dots$, where summation on shared indices is left implicit. In general, $T_{jk} \neq T_{jk}^T = T_{kj}$, hence these expressions do not commute. They therefore represent non-trivial control flow. Conversely, any non-trivial control flow can be written, at any fixed scale or level of abstraction, as a linear sequence of (in general probabilistic) operators. The fixed order of operators in the sequence can be encoded formally by adding “spatial” indices as needed to allow contraction over shared indices. Hence any non-trivial control flow at a fixed scale can be written as a flat TN. This construction can be repeated at each larger scale to produce a hierarchical TN over a collection of “lowest-scale” TNs. \square

We can now examine two corollaries of this result:

Corollary 1. *Decoherent reference sectors exist on \mathcal{B} if and only if control flow can be implemented by a TN.*

Proof. Decoherence sectors require independently-deployable, non-commuting QRFs. This requires a control structure that factors, by Theorem 2 a TN. Conversely, a TN factors the control structure, making QRFs independently deployable, which renders their sectors decoherent. \square

Equivalently, the GM factors if, and only if, control flow can be implemented by a TN.

Corollary 2. *The TN of any system compliant with the FEP is a decomposition of the Identity.*

Proof. The FEP applies to systems with a NESS, and drives such systems to return to (the vicinity of) the NESS after any perturbation. Hence at a sufficiently large scale, the TN of any such system is a cycle, i.e., a decomposition of the Identity. \square

Many standard TN models, e.g., MERAs, assume boundary conditions asymptotically far, in numbers of lowest-scale operators, from the region of the network that is of interest. Identifying such asymptotic boundary conditions yields a cyclic system.

Theorem 2, together with its corollaries, provides a natural, formal means of classifying systems by their control architectures. At a high level, two characteristics distinguish systems with different architectures:

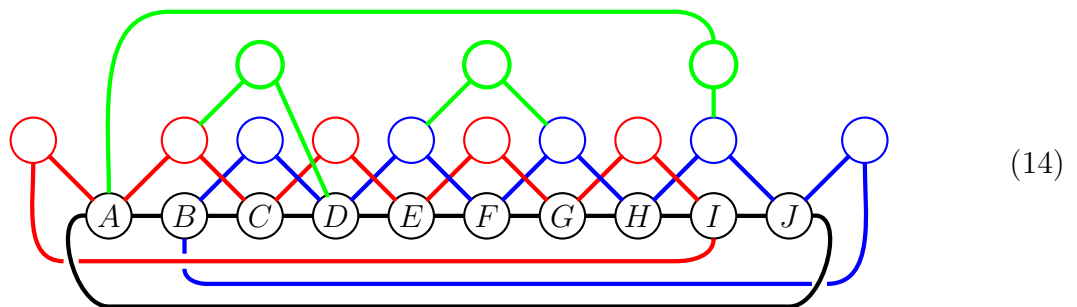
- Hierarchical depth indicates the number of “virtual machine” layers [135] the architecture supports. The interfaces between these layers implement coarse-graining, removing from the higher-level representation all dimensions, and hence all information, which is contracted out of the lower-level operators.
- Number and location of contractions that yield unitary operators, and hence build in entanglement between lower-level operators. The natural limit is a MERA, in which every pair of lower-level operators is entangled at every hierarchical level [48].

The control-flow architecture, in turn, specifies the structure of the “layout” of distinguishable sectors on \mathcal{B} and hence of detectable features/objects in the environment. Locality on \mathcal{B} requires a hierarchical TN; detectable entanglement requires a MERA-like TN. Locality is required for detectable features/objects to appear to have components with nested decomposition. Any QRF for geometric space, and hence for spacetime, must be hierarchical, and must be a MERA if entanglement in space is to be detected. A MERA is required, in particular, if the use of coherence between spatially-separated systems as a computational or communication resource is detectable.

To illustrate the classification of systems by hierarchical level, consider the ten-step cyclic TN shown in Diagram (13):



and its extension to a hierarchy as shown in Diagram (14):



where red, blue, and green colors indicate distinct hierarchical “layers” of tensor contractions. We have trained artificial neural networks (ANNs) to execute these TNs as the sequences of state transitions shown in Table 1. The first sequence (Dataset 1) is a ten-step cycle shown Diagram (13); the second sequence (Dataset 2) layers the coarse-grained state transitions of Diagram (14) onto this ten-step cycle. In Dataset 2, a two-bit tag is used to differentiate the “low-level” from the coarse-grained “high-level” cycles. An example state transition from a randomly-generated initial state is shown in Fig. 2; the red-on-green bit pattern effectively moves “up” one step on each state-transition cycle.

Dataset 1		Dataset 2				
A → B	00	A → B	01	A → C	10	B → D
B → C	00	B → C	01	C → E	10	D → F
C → D	00	C → D	01	E → G	10	F → H
D → E	00	D → E	01	G → I	10	H → J
E → F	00	E → F	01	I → A	10	J → B
F → G	00	F → G				
G → H	00	G → H				
H → I	00	H → I				
I → J	00	I → J				
J → A	00	J → A				

Table 1: Datasets used in ANN simulations. Dataset 1 specifies a ten-step cycle $A \rightarrow B \rightarrow \dots \rightarrow J \rightarrow A$. Dataset 2 specifies this same cycle, with three coarse-grained cycles layered on top. The tags (0,0), (0,1), (1,0), and (1,1) distinguish the data for the low- and high-level cycles.

INPUT (T)											OUTPUT (T+1)										
A	1	1	1	0	0	0	1	0	0	1	B	1	1	1	0	1	1	1	1	0	1
B	1	1	1	0	1	1	1	1	1	0	C	0	1	0	0	1	1	1	0	0	0
C	0	1	0	0	1	1	0	0	0	1	D	1	1	1	1	1	0	0	1	0	1
D	1	1	1	1	1	0	0	0	1	0	E	1	1	0	0	0	0	0	0	0	1
E	1	1	0	0	0	0	0	0	0	1	F	1	1	1	1	0	1	1	0	0	1
F	1	1	1	1	0	1	1	0	0	1	G	1	1	1	0	0	1	1	0	1	0
G	1	1	1	0	0	1	1	0	1	0	H	0	1	0	1	0	0	0	1	0	1
H	0	1	0	1	0	0	0	1	0	1	I	1	0	1	0	0	0	0	1	0	1
I	1	0	1	0	0	0	0	1	0	1	J	0	1	1	1	1	1	1	1	0	1
J	0	1	1	1	1	1	1	1	1	0	A	1	1	1	0	0	0	1	0	0	1

Figure 2: Example state transition from Dataset 1.

We trained two ANNs, one to execute each of the control cycles shown in Table 1. The networks are each composed of three layers, as illustrated in Fig. 3, with network sizes of [10, 50, 10] and [10, 200, 10], respectively, for the input, hidden, and output layers. The units in the hidden layer use the rectified linear unit (ReLU) nonlinear activation function and the neurons in the output layer use the hyperbolic tangent activation function. The network is connected in a feedforward way where a neuron in one layer connects to every neuron in the next layer. Since the ANN serves as a switch state controller, we use a training scheme, similar to one-class classification [136], where the training data are the only data that the network learns to produce. In so doing, the network learns to overfit the training data, and any input outside of the designated state-encoding is discarded. The network is, therefore, not expected to deviate from the learned pattern. The network learns both control regimes wth 100% accuracy after training with 3,000 randomly-generated 10-bit inputs.

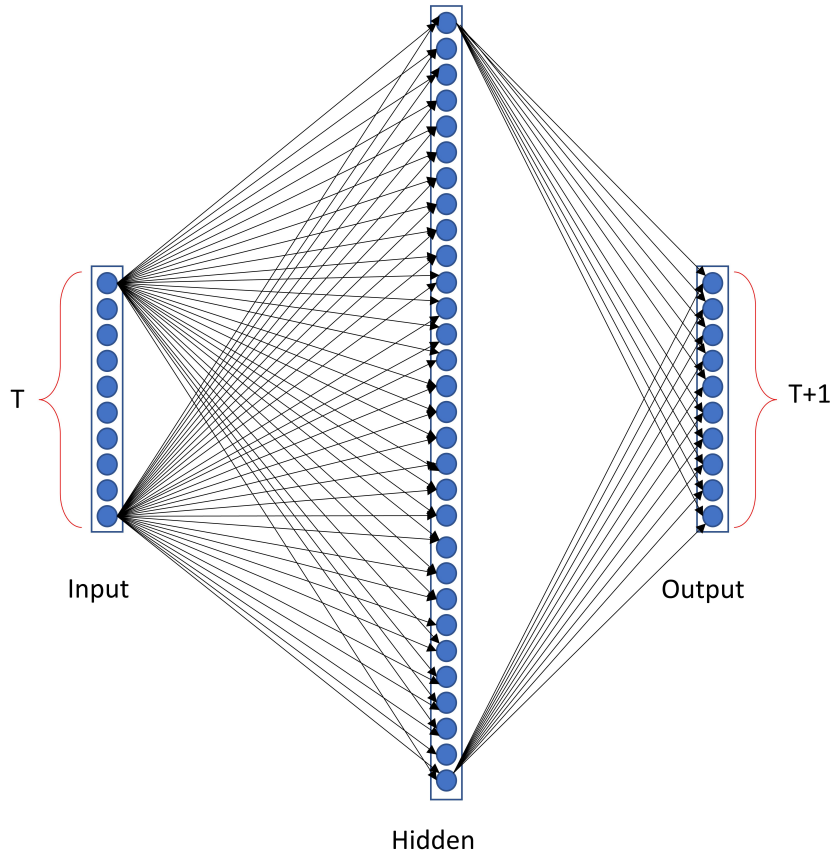


Figure 3: Feed-forward network archtecture used to learn the control cycles specified in Table 1. Each node is connected to every node of the next layer, as shown here for the first and last nodes only. The labels ‘T’ and ‘T+1’ indicate time steps in the executed control flow.

In the more realistic case of noisy input data, where binary states can be flipped, the

Bidirectional Associative Memory (BAM), a minimal two-layer nonlinear feedback network [137], is a viable alternative to a shallow feed-forward ANN. The architecture is shown in Fig. 4. This BAM network learns to associate between the two initial and final states in Table 1, with similar performance to that of the feed-forward network.

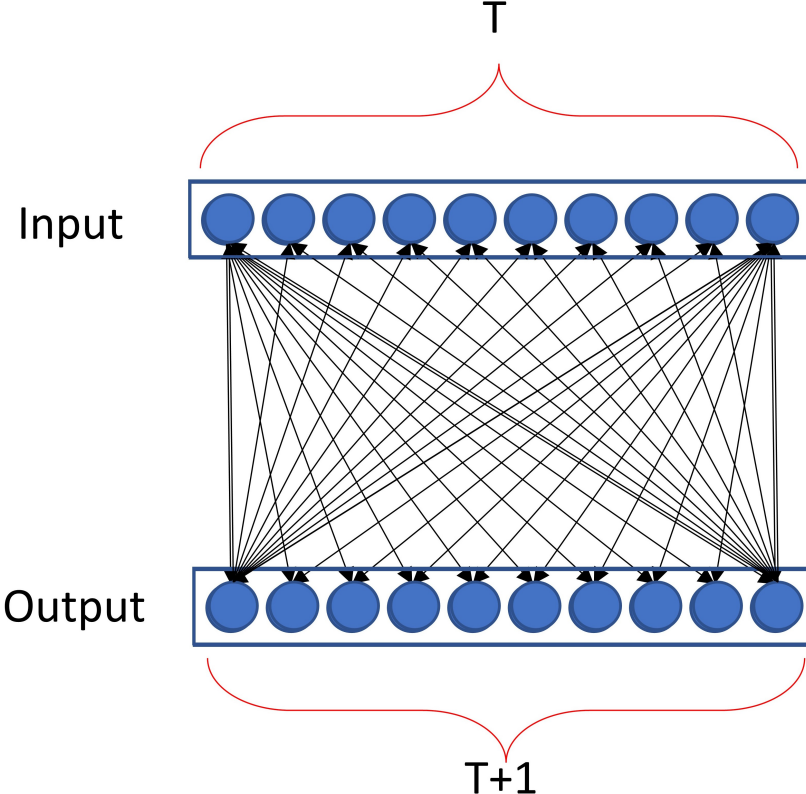


Figure 4: Architecture of the Bidirectional Associative Memory (BAM) network employed here. As in Fig. 3, only the connections of the first and last nodes are shown explicitly.

4 Implementing control flow with TQNNs

Tensor Networks can be naturally associated to the matrix elements of physical scalar products among topological quantum neural networks (TQNNs). Physical scalar products encode indeed the dynamics of TQFTs, since they fulfill their constraints of imposing flatness of the curvature and gauge invariance. Thus, the matrix elements associated to scalar products can be seen as evolution matrix elements for the spin-network states that span the Hilbert spaces of TQNNs.

4.1 Tensor networks as classifiers for TQNNs

A notable example is provided by BF theories [138], a class of TQFTs particularly well studied in the literature of mathematical physics that enables expressing effective theories of particle physics, gravity and condensed matter, and provides as well a general framework for implementations of models of quantum information and quantum computation, machine learning (ML) and neuroscience. These are defined on the principal bundle M of a connection A for some internal gauge group G , with algebra \mathfrak{g} , according to the action on a d -dimensional manifold \mathcal{M}_d

$$\mathcal{S} = \int_{\mathcal{M}_d} \text{Tr}[B \wedge F], \quad (15)$$

where B is an $\text{ad}(\mathfrak{g})$ -valued d -2-form, F denotes the field-strength of A , which is a 2-form, and the trace Tr is over the internal indices of \mathfrak{g} , ensuring gauge invariance of the density Lagrangian $\mathcal{L} = \text{Tr}[B \wedge F]$ of the BF theory.

Variation with respect to the conjugated variables, the connection A and the B frame-field, closing a canonical symplectic structure, provide the equations of motion of the theory [138]:

$$F = 0, \quad d_A B = 0, \quad (16)$$

respectively the curvature constraint, imposing the flatness of the connection, and the Gauß constraint, imposing invariance under gauge transformations, having denoted with d_A the covariant derivative with respect to the connection A .

At the quantum level, the states of the kinematical Hilbert space of the theory, fulfilling by construction the Gauß constraint, can be represented in terms of cylindrical functionals Cyl , supported on graphs Γ that are unions of segments γ_i , the end points of which meet in nodes n , and with holonomies – elements of the group $G - H_{\gamma_i}[A]$ of the connection A assigned to γ_i and intertwiner operators – invariant tensor product of representations – v_n assigned to the nodes n .

For $G = \text{SU}(2)$, spin-networks $|\Gamma, j_\gamma, \iota_n\rangle$, supported on Γ and labelled by the spin j_γ of the irreducible representations of the group elements assigned to γ and by the quantum intertwiner numbers ι_n associated to v_n , represent a basis of the kinematical Hilbert space of the theory. In terms of functionals of Cyl , one can provide the holonomy representation, which is related to the “spin and intertwiner” representation of $|\Gamma, j_\gamma, \iota_n\rangle$ by means of the Peter-Weyl transform. This allows us to decompose the spin-network cylindric functional as [139]:

$$\Psi_{j_{\gamma_{ij}}, \iota_{n_i}}(h_{\gamma_{ij}}) = \left(\bigotimes_n \iota_n \right) \cdot \left(\bigotimes_{\gamma_{ij}} D^{(j_{\gamma_{ij}})}(h_{\gamma_{ij}}) \right), \quad (17)$$

with $D^{(j)}$ are Wigner matrices providing representation matrices of the $\text{SU}(2)$ group elements.

The functorial evolution among spin-networks is ensured by the projector operator [140], which implements the curvature constraint in the physical scalar product among states, i.e.

$$\langle \text{in} | P | \text{out} \rangle, \quad \text{with} \quad P = \int \mathcal{D}[N] \exp(i \int \text{Tr}[NF]). \quad (18)$$

We may then regard $|\text{in}\rangle$ as elements of the Hilbert space, and without loss of generality pick up those ones resulting from composing tensorially in *Cyl k*-representations of holonomies. We may further denote them as $|j_1 \dots j_k\rangle$, with some ordering prescription to associate the topological structure of Γ to the sequence of spin labels. Physically evolving states $P|\text{in}\rangle$ are distinguished from the former ones by labelling them as $|\widetilde{j}_1 \dots j_k\rangle$. Similarly, we introduce $|\text{out}\rangle$ as the tensor product of $(n-k)$ -representations of holonomies, and denote these states as $|i_1 \dots i_{n-k}\rangle$. Then the matrix elements of $\langle \text{in} | P | \text{out} \rangle$ naturally give rise [98] to an n -tensor, i.e.

$$\langle i_1 \dots i_{n-k} | \widetilde{j}_1 \dots j_k \rangle = T_{i_1 \dots i_{n-k} j_1 \dots j_k}. \quad (19)$$

4.2 Geometric RG flow for TQNNs and TNs

The mathematical structures of TQNNs we summarized in Sec. 4.1 are picturing systems “at equilibrium”, for which TQFTs characterize a topological stability that percolates into the related transition amplitudes. Nonetheless, it is worth considering as well how stochastic noise might interfere with the topological order ensured by TQFTs, and study the role of “out-of-equilibrium” physics in the analysis of the evolution of the systems under scrutiny.

Out-of-equilibrium dynamics is instantiated considering a heat-flow evolution of the fundamental fields of the theory, with respect to a thermal time τ . Typical Langevin equations, complemented with stochastic noise, provide through their convergence toward the equations of motion of the theory the relaxation toward equilibrium of the field configurations representing specific systems [141]. In general, given some fields ϕ_σ , with a classical equation of motion derived, according to the variational principle $\delta\mathcal{S}/\delta\phi_\sigma$, from an action \mathcal{S} over a Euclidean manifold \mathcal{M} , the associated Langevin equations read:

$$\frac{\partial}{\partial \tau} \phi_\sigma = -\frac{\delta\mathcal{S}}{\delta\phi_\sigma} + \eta_\sigma, \quad (20)$$

with η_σ a stochastic noise term. The theory at equilibrium is characterized by the symmetries of the equations of motion $\delta\mathcal{S}/\delta\phi_\sigma = 0$ that are broken in the transient phase [142]; these symmetries are consistent with – and in the case of BF theories, actually generated by – the theories at equilibrium.

A prototype of geometric heat-flow was introduced by Hamilton, and then used by Perelman to prove the Poincaré conjecture, which goes under the name of Ricci flow. Here the gravitational field $g_{\mu\nu}$ is the basic configurational space field, while the drift terms are the Einstein equations of motion in the vacuum, which indeed are expressed by requiring that

the components of the Ricci tensor vanish, i.e. $R_{\mu\nu} = 0$. The Ricci flow then reads

$$\imath \frac{\partial}{\partial \tau} g_{\mu\nu} = -2R_{\mu\nu}, \quad (21)$$

having considered now a Lorentzian manifold \mathcal{M} . The Ricci flow equations can be further complemented introducing the Ricci target $R_{\mu\nu}^T = \kappa^2(T_{\mu\nu} - 1/2g_{\mu\nu}T)$, expressed in terms of the Newton constant $G = \kappa^2/(8\pi)$ and the energy-momentum tensor of matter $T_{\mu\nu}$, so as to obtain at equilibrium the Einstein equations:

$$R_{\mu\nu} - \frac{1}{2}g_{\mu\nu}R = \kappa^2T_{\mu\nu}, \quad \text{or equivalently} \quad R_{\mu\nu} = R_{\mu\nu}^T. \quad (22)$$

The stochastic version of the Ricci flow, with heat equation turning into a Langevin equation, has been introduced and deepened in [142] for a generic gravitational system in the presence of matter fields, describing an action \mathcal{S} for gravity and matter. Moving then from:

$$\imath \frac{\partial}{\partial \tau} g_{\mu\nu} = -\frac{1}{\kappa^2} \frac{\delta \mathcal{S}}{\delta g^{\mu\nu}} + \eta g_{\mu\nu}, \quad (23)$$

in which a multiplicative noise $\eta_{\mu\nu} = \eta g_{\mu\nu}$ appears, the Hamiltonian analysis of the stochastic Ricci flow (SRF) in the Adomian decomposition method (ADM) variables has been derived [142].

An essential by-product of the discussion, from the Ricci flow perspective, is that the equilibration trajectories corresponds to those of a renormalization group (RG) flow. The thermal time τ plays the role of scale parameter that individuates a dimension in the bulk, which is out-of-equilibrium. The boundaries are recovered asymptotically in τ , in the infra-red regime, and are by definition at equilibrium and thus symmetric.

For a particular class of TQFTs, the BF theories we have introduced in Sec. 4.1 for implementing TQNNs and TNs, the geometric RG flow acquire a specific expression as the TQFT equivalent of the gravitational Ricci flow [143].

4.3 TNs as a generalization of the main model architectures in ML

The use of TNs is an emerging topic in the ML community. The integration between the two appears quite immediate. A TN structure can be viewed as an ML model in which the parameters are properly adjusted to learn the classification of a data set. Yet, as Ref. [144] mentions, machine learning can aid, in turn, in determining a factorization of a TN approximating a data set. Moreover, TNs are also used to compress the layers of ANN architectures, besides a variety of other uses. Tensor networks are becoming more and more popular to the extent that they are a powerful tool for representing and manipulating high-dimensional data, as in the case of image and video classification tasks in which the data is represented as a high-dimensional tensor. High efficiency, flexibility, and easy to

use are making them a dominant choice for many AI applications. Furthermore, besides being used to represent data, TNs can be used to process data by exploiting a number of operators. This feature makes them an effective technique for processing data in ML applications.

As it is well known, TNs are particularly well suited for representing quantum many-body states in which the dimension of the Hilbert space is exponentially large in the number of particles. The corresponding ML approach consists in:

- Lifting data to exponentially higher spaces;
- Applying any linear classifier $f(x) = W^* \Phi(X)$ to a non-linear space;
- Compressing the weights by using TNs.

The output of the model is a separation of classes that would not be linearly separable in a linear space. In particular, the decision function is the overlap of the weight tensor W with the feature map tensor Φ as in Fig. 5. The weight tensor W can be approximated by the decomposition in Fig. 6.

$$f(\mathbf{x}) = \begin{array}{c} \text{---} \\ | \\ | \\ | \\ | \\ | \end{array} \quad W \quad \Phi(\mathbf{x})$$

Figure 5: Representation of the decision function (see [145]).

$$\begin{aligned} W &= \text{---} && \text{order-}N \text{ tensor} \\ &\approx \begin{array}{cccccc} | & | & | & | & | & | \end{array} && \begin{array}{l} \text{matrix} \\ \text{product} \\ \text{state (MPS)} \end{array} \end{aligned}$$

Figure 6: Matrix product decomposition (again see [145]).

Regularization and optimization are built as a constructive product of low-order tensors while weight compression is performed by using the Matrix Product States (MPS) decomposition. If we look at Deep Neural Networks as a piecewise composition of linear

discriminators (logistic regression functions), then the TN framework appears as a generalization of the main model architectures found in the ML literature, e.g. Support Vector Machines, Kernel models, and Deep Neural Networks.

The literature concerning the use of tensor theory in traditional ML is becoming large. A short review starts with a seminal paper by Stoudenmire and Schwab [146], which demonstrated how algorithms for optimizing TNs can be adapted to supervised learning tasks by using MPS (tensor trains) to parametrize non-linear kernel learning models. Novikov, Trofimov, and Oseledets [147] have shown how an exponentially large tensor of parameters can be represented in a factorized format called Tensor Train (TT), with the consequence of obtaining a regularization of the model. van Glasser, Pancotti, and Cirac [148] explored the connection between TNs and probabilistic graphical models by introducing the concept of a “generalized tensor network architecture” for ML. Ref. [149] then designed a generative model, i.e. a traditional machine learning model that learns joint probability distributions from data and generates samples according to it, by using MPS. Ref. [150] made use of autoregressive MPSs for building an unsupervised learning model that goes beyond proof-of-concept by showing performance comparable to standard traditional models. Finally, Ref. [151] analyzes the contribution of polynomials of different degrees to the supervised learning performance of different architectures.

5 Implications for biological control systems

Scale-free biology requires a smooth transition from quantum-like to classical-like behavior. Typical representations of metabolic, signal-transduction, and gene-regulatory pathways are entirely classical, even though many of their steps involve electron-transfer or other mechanisms that are acknowledged to require a quantum-theoretic description [87, 152]. As noted earlier, free-energy budget considerations suggest that both prokaryotic and eukaryotic cells employ quantum coherence as a computational resource [92]. Emerging empirical evidence for longer-range entanglement in mammalian brains suggests that large-scale networks may also be using quantum coherence as a resource [93]. Control flow models must, therefore, support the possibility of quantum computation in biological systems. Hierarchical TNs that include unitary components, e.g., MERA-type models, provide this capability.

In prokaryotes, the primary tasks of control flow are adapting metabolism to available resources via metabolite-driven gene regulation [153] and initiating DNA replication and cell division when conditions are favorable. We can, therefore, expect shallow hierarchies of effectively classical control transitions in these organisms. Eukaryotes, however, are characterized by both intracellular compartmentalization and morphological degrees of freedom at the whole-cell scale. We have shown previously that the FEP will induce “neuromorphic” morphologies – i.e. morphologies that segregate inputs from outputs and enable a fan-in/fan-out computational architecture – in any systems with morphological degrees of freedom [154]. Such systems can be expected to have deep control hierarchies at the cellular level, with hierarchical structure correlating with morphological structure

in morphologically-complex cells such as neurons [155], and in multicellular assemblages at all scales. As well as managing metabolism and replication, such systems must implement active exploration of the environment, communication with other systems, and – crucially for cognition – the writing and reading of stigmergic memories. Thus we can expect such systems to implement QRFs for spacetime and for specific kinds of objects, e.g., conspecifics and suitable substrates for recording stigmergic memories. Such QRFs rely on symmetries, and hence on redundancy of encoded (or encodable) information; they depend, in other words, on the availability of error-correcting codes [25, 156]. The implementation of spacetime as a quantum error-correcting code by TNs has been extensively studied by physicists; see [157] for review and [98] for a detailed analysis using the present formalism. The use of spacetime as an error-correcting code by organisms – e.g., the implementation of translational and rotational invariance of objects by dorsal visual processing in mammals [158, 159] – is well-understood phenomenologically, but the details of neural implementation remain to be elucidated.

Both the context-sensitivity of, and the occurrence of context effects due to non-commutativity of QRFs in, control networks can be expected to increase with their complexity and hierarchical depth. “Bowtie” networks with high fan-in/fan-out to/from multi-use proteins or second messengers such as Ca^{2+} are increasingly recognized as ubiquitous in high eukaryotic cells [160]. Such networks have the general form of the CCCD depicted in Diagram (3). Frequently, such networks evolve via compression of information (e.g. toward shared second messengers, as in $[\text{Ca}^{2+}]$ -based interactions [161, 162]) as an efficiency-increasing mechanism. Bowties introduce semantic ambiguities that must be resolved by context. Each incoming signal has its own governing semantics, but the relevant context can depend on boundary conditions which can be exceedingly difficult (if not impossible) to predetermine (see e.g., [163, 164] for general discussions of the history and semantic depth of this problem). As pointed out in [22], a context change $x \mapsto y$ is semantically problematic if for a fixed set $\{o_i\}$ of observations, the conditional probability distributions $P(o_i|x)$ and $P(o_i|y)$ are well defined, but the joint distribution $P(o_i|x \vee y)$ is not [106]. This occurs whenever the QRFs for x and y do not commute [57, Th 7.1]. As suggested by Diagram (3), this context-switching problem affects deep learning using VAEs [165]; see e.g., the application to antimicrobial peptides in [166]. In general, the structure of Diagram (3) can serve as a convenient benchmark for distinguishing signal transduction networks that incorporate co-deployable versus non-co-deployable QRFs [57].

“Quantum” context effects due to non-commutativity have, interestingly, been reported even at the scale of human language use. The “Snow Queen” experiment [167] challenged subjects with distinct, mutually-inconsistent meanings of terms such as ‘kind’, ‘evil’, or ‘beautiful’ in different contexts, and detected statistically-significant context effects using the CbD formalism [62, 63]. Such effects cannot be explained by linguistic ambiguity, misreading, etc. Such language-driven contextuality is taken up in the setting of psycholinguistics and distributional semantics in [168], which combines CbD and the sheaf theoretic [60, 61] methods to systematically study semantic ambiguity as creating meaning/sense discrepancies in statements like “It was about time”, “She had time on her hands to win

the heat”, “West led with a queen”, etc.

While the notion of “languages” has thus far been applied to cells, tissues, and even non-vertebrates in a mostly metaphorical way, we can speculate that linguistic approaches to understanding the interplay between context dependence and semantic ambiguity may be useful to biology in general. Immune cells (e.g., T cells) are, for example, “programmed” or “trained” by their progenitor cells to respond to local cellular signals and ambient conditions in particular ways. Unexpected context changes may induce dysfunctional (at the organism scale) responses, including chronic disorders [169]; these can be considered consequences of discrepancies between the “actual” semantics of incoming signals and the semantics expected by the immune systems’ “language.” This suggestion of possible “linguistic” contextuality seems in consonance with the hypothesis of [170] that the immune system is a cognitive (living) system implementing its exclusive system of language-grammar, which may be prone to analogous disorders of communication as those discussed in [168]. Similar context effects have been observed in microbiological systems [171]; here discrepancies in experimentally derived classical probabilities arising from lactose-glucose interference signaling in *E. Coli* can only be explained in terms of non-classical probabilities. We note that the expression ‘quantum-like’ [172] is often used for such effects; however, their formal structure is exactly that given by quantum theory.

We expect that further research into quantum biology will unfold significant perspectives on human/mammalian physiology and cognitive capabilities along the lines suggested in the present article. For example, allostatic maintenance, as briefly alluded to in §2.1, can be seen as a process regulating a body’s physiological conditions relative to costs and benefits while dynamically allocating resources for the purpose of overall adaptability of an organism within its internal environment. Implementing the allostatic and anticipatory mechanisms are the visceromotor cortical regions generating autonomic, hormonal, and immunological predictions leading to interoceptive inference [68, 69, 70, 82, 173, 174, 176, 177]. This process of inference in humans and mammals putatively utilizes predictive coding for the processes of homeostasis-allostasis through a hierarchy of cellular to organ-level systems, in turn connecting interoception to the processes of exteroception and proprioception [82, 173, 177, 178, 179]. The basic principles follow from how allostasis provides protection against potential surprise by utilizing a framework somewhat beyond the error signaling necessary for homeostatic maintenance (it is essentially through minimizing the free energy of internal state trajectories towards combatting surprise, as discussed in §2.1). The net effect of the process is consonant with the Good Regulator theorem of [175], showing how regulation of a given system requires an internal model of that system. A further perspective is to emphasize the predictive nature of an integrated, complex, allostatic-interoceptive cortical system capable of supporting a spectrum of psychological phenomena including memory and emotions [177] (cf. [82]). Accordingly, cognitive conditions such as depression and autism have been described as abnormalities of allostatic-interoceptive inference, so impairing predictive coding mechanisms due to aberrant assimilation and mistuning of prediction errors (putatively a connectivity issue), conceivably leading to a root cause of many known cognitive conditions [82, 173, 178].

We anticipate that this fully general, context sensitive model of control flow will be important for understanding morphogenesis, which is not simply a feed-forward emergent system, but rather a highly context-sensitive error-minimizing process [23]. Specifically, the collective intelligence of cells during embryonic development, organ regeneration, and metamorphosis can create and repair specific complex structures despite a wide range of perturbations [180]. Changes in the genome, the number of cells, or the starting configuration can often be overcome: bisected embryos result in normal twins, amputated salamander limbs re-grow back to normal, and planarian fragments result in perfect little worms [181]. The competency of cellular collectives to reach the correct target morphology despite even drastic interventions requires an understanding of how they navigate, via context-sensitive control flow, problem spaces including anatomical morphospace [182], physiological, and transcriptional spaces [156, 183]. Understanding the navigation policies used by unconventional collective intelligences can help not only understand creative problem-solving on rapid timescales (such as the ability to regulate genes to accommodate an entirely novel stressor [184] without evolutionary adaptation), but may also have implications for predicting and managing the goals and behavioral repertoires of synthetic beings [185].

6 Conclusion

We have shown here how the problem of defining control flow arises in active inference systems, and provided three formal representations of the problem. We have proved that control flow in such systems can always be represented by a tensor network, provided illustrative examples, and shown how the general formalism of topological quantum neural networks can be used to implement a general model of control flow. These results provide a general formalism with which to characterize context dependence in active inference systems at any scale, from that of macromolecular pathways to that of multi-organism communities. They suggest that the concept of communication by language is not just metaphorical when applied to biological systems in general, but rather an appropriate and productive description of interactional dynamics.

We view these results as a further step toward fully integrating the formal models, concepts, and languages of physics, biology, and cognitive science. This integration is not reductive. It rather allows us to classify systems using natural measures of organizational and computational complexity, and to understand how interactions between simpler systems can implement the more complex behavior of the larger systems that they compose.

Acknowledgements

K.F. is supported by funding for the Wellcome Centre for Human Neuroimaging (Ref: 205103/Z/16/Z), a Canada-UK Artificial Intelligence Initiative (Ref: ES/T01279X/1) and the European Union’s Horizon 2020 Framework Programme for Research and Innovation

under the Specific Grant Agreement No. 945539 (Human Brain Project SGA3). M.L. gratefully acknowledges funding from the Guy Foundation and the John Templeton Foundation, Grant 62230. A.M. wishes to acknowledge support by the Shanghai Municipality, through the grant No. KBH1512299, by Fudan University, through the grant No. JJH1512105, the Natural Science Foundation of China, through the grant No. 11875113, and by the Department of Physics at Fudan University, through the grant No. IDH1512092/001.

Conflict of interest

The authors declare no competing, financial, or commercial interests in this research.

References

- [1] Friston KJ. A theory of cortical responses. *Philos Trans R Soc Lond B, Biol Sci* 2005;360:815–36.
- [2] Friston KJ, Kilner J, Harrison L. A free energy principle for the brain. *J Physiol Paris* 2006;100:70–87.
- [3] Friston KJ, Stephan KE. Free-energy and the brain. *Synthese* 2007;159:417–58.
- [4] Friston, K. J. 2010 The free-energy principle: A unified brain theory? *Nature Reviews Neuroscience* 11, 127–138.
- [5] Friston, K. J. 2013 Life as we know it. *Journal of The Royal Society Interface* 10, 20130475.
- [6] Friston KJ, Fitzgerald T, Rigoli F, Schwartenbeck P, Pezzulo G. Active inference: a process theory. *Neural Comput* 2017;29:1–49.
- [7] Ramstead MJ, Badcock PB, Friston KJ. Answering Schrödinger’s question: a free-energy formulation. *Phys Life Rev* 2018;24:1–16.
- [8] Ramstead MJ, Constant A, Badcock PB, Friston KJ. 2019 Variational ecology and the physics of sentient systems. *Phys. Life Rev.* 31, 188–205.
- [9] Kuchling F, Friston K, Georgiev G, Levin M. 2020 Morphogenesis as Bayesian inference: A variational approach to pattern formation and control in complex biological systems. *Phys Life Rev* 33, 88–108.
- [10] Friston, K. J. 2019 A free energy principle for a particular physics. Preprint arXiv:1906.10184 [q-bio.NC]. <https://arxiv.org/abs/1906.10184>

- [11] Ramstead MJ, Sakthivadivel DAR, Heins C, Koudahl M, Millidge B, Da Costa L, Klein B, Friston KJ 2022 On Bayesian mechanics: A physics of and by beliefs. Preprint arXiv:2205.11543 [cond-mat.stat-mech].
- [12] Fields C, Friston K, Glazebrook JF, Levin M 2022 A free energy principle for generic quantum systems. *Prog. Biophys. Mol. Biol.* 173, 36–59.
- [13] Friston, K., Da Costa, L., Sakthivadivel, D. A. R., Heins, C., Pavliotis, G. A., Ramstead, M., Parr, T. 2022 Path integrals, particular kinds, and strange things. Preprint arXiv:2210.12761.
- [14] Pearl, J. 1988 *Probabilistic Reasoning in Intelligent Systems: Networks of Plausible Inference*. San Mateo CA: Morgan Kaufmann.
- [15] Clark A. 2017 How to knit your own Markov blanket: Resisting the second law with metamorphic minds. In (T. Wetzinger and W. Wiese, eds.) *Philosophy and Predictive Processing 3*, 19pp. Frankfurt am Main: Mind Group.
- [16] Kirchhoff, M., Parr, T., Palacios, E., Friston, K., Kiverstein, J. 2018 The Markov blankets of life: Autonomy, active inference and the free energy principle. *J. R. Soc. Interface* 15, 20170792.
- [17] Parr, T., Da Costa, L., Friston, K. 2020 Markov blankets, information geometry and stochastic thermodynamics. *Philos. Trans. A: Math. Phys. Eng. Sci.* 378, 20190159.
- [18] Sakthivadivel, D.A.R. 2022 Weak Markov blankets in high-dimensional, sparsely-coupled random dynamical systems. Preprint arXiv:2207.07620.
- [19] Wheeler, J. H. 1989 Information, physics, quantum: The search for links. In: Zurek, W. (Ed.), *Complexity, Entropy, and the Physics of Information*. CRC Press, Boca Raton, FL, pp. 3–28.
- [20] Levin, M. 2019 The computational boundary of a “self”: Developmental bioelectricity drives multicellularity and scale-free cognition. *Front. Psychol.* 10, 1688.
- [21] Levin, M. 2021 Life, death, and self: Fundamental questions of primitive cognition viewed through the lens of body plasticity and synthetic organisms. *Biochem. Biophys. Res. Commun.* 564, 114–133.
- [22] Fields, C.; Glazebrook, J. F.; Levin, M. 2021 Minimal physicalism as a scale-free substrate for cognition and consciousness. *Neurosci. Cons.* 7(2), niab013.
- [23] Levin, M. 2022 Technological approach to mind everywhere: An experimentally-grounded framework for understanding diverse bodies and minds. *Front. Syst. Neurosci.* 16, 768201.
- [24] Endsley, M. R. 2012 Situational awareness. In: Salvendy, G. (Ed.) *Handbook of Human Factors and Ergonomics*, 4th Ed. Hoboken, NJ, John Wiley, pp. 553–568.

- [25] Fields, C.; Levin, M. 2018 Multiscale memory and bioelectric error correction in the cytoplasm-cytoskeleton-membrane system. *WIREs Syst. Biol. Med.* 10, e1410.
- [26] Clark, A., Chalmers, D. 1998 The extended mind (Active externalism). *Analysis* 58(1), 7–19.
- [27] Anderson, M. L. 2003 Embodied cognition: A field guide. *Artif. Intell.* 149, 91–130.
- [28] Froese, T., Ziemke, T 2009 Enactive artificial intelligence: Investigating the systemic organization of life and mind. *Artif. Intell.* 173, 466–500.
- [29] Attias, H. 2003 Planning by probabilistic inference. *Proc. of the 9th Int. Workshop on Artificial Intelligence and Statistics* in Proc. Machine Learning Res. R4, 9–16.
- [30] Botvinick, M., Toussaint, M. 2012 Planning as inference. *Trends Cogn. Sci.* 16(10), 485–488.
- [31] Lanillos, P., Mio, C., Pezzato, C., et al. 2021 Active inference in robotics and artificial agents: Survey and challenges. Preprint arXiv:2112.01871.
- [32] Chubukov, V., Gerosa, L., Kochanowski, K., Sauer, U. 2014 Coordination of microbial metabolism. *Nat. Rev. Microbiol.* 12, 327–340.
- [33] Micali, G., Endres, R. G. 2016 Bacterial chemotaxis: information processing, thermodynamics, and behavior. *Curr. Opin. Microbiol.* 30, 8–15.
- [34] Pezzulo, G., LaPalme, J., Durant, F., Levin, M. 2021 Bistability of somatic pattern memories: stochastic outcomes in bioelectric circuits underlying regeneration. *Philos. Trans. R. Soc. Lond. B* 376(1821), 20190765.
- [35] Blake, R., Logothetis, N. K. 2002 Visual competition. *Nat. Rev. Neurosci.* 3, 1–11.
- [36] Stertzer, P., Kleinschmidt, A., Rees, G. 2009 The neural bases of multistable perception. *Trends Cogn. Sci.* 13, 310–318.
- [37] Schwartz, J.-L., Grimault, N., Hupé, J.-M., Moore, B. C. J., Pressnitzer, D. 2012 Multistability in perception: bindingsensory modalities, An overview. *Phil. Trans. R. Soc. Lond. B* 367, 896–905.
- [38] Vossel, S., Geng, J. J., Fink, G. R. 2014 Dorsal and ventral attention systems: Distinct neural circuits but collaborative roles. *Neuroscientist* 20, 150–159.
- [39] Baars, B. J., Franklin, S. 2003 How conscious experience and working memory interact. *Trends Cogn. Sci.* 7, 166–172.
- [40] Baars, B. J., Franklin, S., Ramsoy, T. Z. 2013 Global workspace dynamics: Cortical “binding and propagation” enables conscious contents. *Front. Psychol.* 4, 200.

- [41] Kuchling, F.; Fields, C.; Levin, M. 2022 Metacognition as a consequence of competing evolutionary time scales. *Entropy* 24, 601.
- [42] Parr, T., Friston, K. J. 2019 Generalised free energy and active inference. *Biol. Cybern.* 113(5-6), 495–513.
- [43] Winn, J. Bishop, C. M. 2005 Variational message passing. *J. Mach. Learn. Res.* 6, 661–694.
- [44] Dauwels, J. 2007 On variational message passing on factor graphs. *2007 IEEE International Symposium on Information Theory*, Nice, France.
- [45] Parr, T., Sajid, N., Friston, K. J. 2020 Modules or mean-fields? *Entropy* 22(5), 552.
- [46] Da Costa, L., Parr, T. Sajid, N., Veselic, S., Neacsu, V., Friston, K. 2020 Active inference on discrete state-spaces: A synthesis. *J. Math. Psychol.* 99, 102447.
- [47] Friston, K., Parr, T., de Vries, B. 2017 The graphical brain: Belief propagation and active inference. *Netw. Neurosci.* 1(4), 381–414.
- [48] Orús, R. 2019 Tensor networks for complex quantum systems. *Nat. Rev. Phys.* 1, 538–550.
- [49] Bao, N., Cao, C.-J., Carroll, S. M., Chatwin-Davies, A. 2017 de Sitter space as a tensor network: Cosmic no-hair, complementarity, and complexity. *Phys. Rev. D* 96, 123536.
- [50] Hu, Q., Vidal, G. 2017 Spacetime symmetries and conformal data in the continuous Multiscale Entanglement Renormalization Ansatz. *Phys. Rev. Lett.* 119, 010603.
- [51] Chandra, A. R., de Boer, J., Flory, M., Heller, M. P., Hörtner, S., Rolph, A. 2021 Spacetime as a quantum circuit. *J. High Energy Phys.* 2021, 207.
- [52] Aharonov Y, Kaufherr T. Quantum frames of reference. *Phys Rev D* 1984;30:368–385.
- [53] Bartlett SD, Rudolph T, Spekkens RW. 2007 Reference frames, super-selection rules, and quantum information. *Rev Mod Phys* 79, 555–609.
- [54] Barwise, J.; Seligman, J. 1997 *Information Flow: The Logic of Distributed Systems* (Cambridge Tracts in Theoretical Computer Science 44). Cambridge University Press, Cambridge, UK.
- [55] Fields, C.; Glazebrook, J. F. 2019 A mosaic of Chu spaces and Channel Theory I: Category-theoretic concepts and tools. *J. Expt. Theor. Artif. intell.* 31, 177–213.
- [56] Fields, C.; Glazebrook, J. F. 2020 Representing measurement as a thermodynamic symmetry breaking. *Symmetry* 12, 810.

- [57] Fields, C.; Glazebrook, J. F. 2022 Information flow in context-dependent hierarchical Bayesian inference. *J. Expt. Theor. Artif. intell.* 34, 111–142.
- [58] Fields, C.; Glazebrook, J. F.; Marcianò, A. 2021 Reference frame induced symmetry breaking on holographic screens. *Symmetry* 13, 408.
- [59] Fields, C.; Glazebrook, J. F.; Marcianò, A. (2022) Sequential measurements, topological quantum field theories, and topological quantum neural networks. *Fortschr. Phys.* 2022, 2200104.
- [60] Abramsky, S., Brandenburger, A. 2011 The sheaf-theoretic structure of non-locality and contextuality. *New J. Phys.* 13, 113036.
- [61] Abramsky, S., Barbosa, R. S., Mansfield, S. 2017 Contextual fraction as a measure of contextuality. *Phys. Rev. Lett.* 119, 050504.
- [62] Dzhafarov, E. N.; Kujala, J. V. (2017a). Contextuality-by-Default 2.0: Systems with binary random variables. In: J. A. Barros, B. Coecke and E. Pothos (eds.) *Lecture Notes in Computer Science* 10106, Springer, Berlin, 16–32.
- [63] Dzhafarov, E. N. & Kon, M. 2018 On universality of classical probability with contextually labeled random variables. *J. Math. Psychol.* 85, 17–24.
- [64] Adlam, E. 2021 Contextuality, fine-tuning and teleological explanation. Preprint arXiv:2110.15898v2 [quant-ph].
- [65] Marcianò, A.; Chen, D.; Fabrocini, F.; Fields, C.; Greco, E.; Gresnigt, N.; Jinklub, K.; Lulli, M., Terzidis, K.; Zappala, E. 2022 Quantum neural networks and topological quantum field theories. *Neural Networks* 153, 164–178.
- [66] Marcianò, A., Chen, D., Fabrocini, F., Fields, C., Lulli, M., Zappala, E. 2022 Deep neural networks as the semi-classical Limit of topological quantum neural networks: The problem of generalisation. Preprint arXiv:2210.13741.
- [67] Sterling, P., Eyer, J. 1988 Allostasis: A new paradigm to explain arousal pathology. In: *Handbook of Life Stress, Cognition and Health*. John Wiley & Sons: New York, pp. 629–649.
- [68] Barrett, L. F., Quigley, K. S., Hamilton, P. 2016 An active inference theory of allostasis and interoception in depression. *Philos. Trans. R. Soc. Lond. B Biol. Sci.* 371(1708), 20160011.
- [69] Corcoran, A. W., Pezzulo, G., Hohwy, J. 2020 From allostatic agents to counterfactual cognisers: Active inference, biological regulation, and the origins of cognition. *Biol. Philos.* 35(3), 32.
- [70] Hohwy, J. 2016 The self-evidencing brain. *Nous* 50(2), 259–285.

- [71] Sakthivadivel, D. A. R. 2022 A constraint geometry for inference and integration. Preprint arXiv:2203.08119.
- [72] Sakthivadivel, D. A. R. 2022 Towards a geometry and analysis for Bayesian mechanics. Preprint arXiv:2204.11900.
- [73] Landauer, R. 1961 Irreversibility and heat generation in the computing process. *IBM J. Res. Dev.* 5, 183–195.
- [74] Jarzynski, C. 1997 Nonequilibrium equality for free energy differences. *Phys. Rev. Lett.* 78(14), 2690–2693.
- [75] Evans, D. J. 2003 A non-equilibrium free energy theorem for deterministic systems. *Molec. Phys* 101(10), 1551–1554.
- [76] Friston, K., Thornton, C., Clark, A. 2012 Free-energy minimization and the dark-room problem. *Front. Psychol.* 3, 130.
- [77] Pezzulo, G., Rigoli, F., Friston, K. 2015 Active Inference, homeostatic regulation and adaptive behavioural control. *Prog. Neurobiol.* 134, 17–35.
- [78] Friston, K., Rigole, F., Ognibene, D., Mathys, C., Fitzgerald, T., Pezzulo, G. 2015 Active inference and epistemic value. *Cogn. Neurosci.* 6, 187–214.
- [79] Schmidhuber, J. 1991 Curious model-building control-systems. *1991 IEEE International Joint Conference on Neural Networks*, Vols 1-3; 2, 1458–1463.
- [80] Sun, Y., Gomez, F., Schmidhuber, J. 2011 Planning to be surprised: Optimal Bayesian exploration in dynamic environments. *Artificial General Intelligence*. J. Schmidhuber, K. R. Thórisson and M. Looks, Eds. Berlin, Heidelberg, Springer. pp. 41–51.
- [81] Sengupta, B., Friston, K. 2018 How Robust are deep neural networks? Preprint arXiv arXiv:1804.11313.
- [82] Seth, A. K., Friston, K. J. 2016 Active interoceptive inference and the emotional brain. *Philos. Trans. R. Soc. Lond. B* 371(1708), 20160007.
- [83] Emmons-Bell, M., Durant, F., Hammelman, J. et al. 2015 Gap junctional blockade stochastically induces different species-specific head anatomies in genetically wild-type *Girardia dorotocephala* flatworms. *Int. J. Mol. Sci.* 16, 27865–27896.
- [84] Oviedo, N. J., J. Morokuma, Walentek, P. et al. 2010 Long-range neural and gap junction protein-mediated cues control polarity during planarian regeneration. *Dev. Biol.* 339, 188–199.
- [85] Tegmark M 2000 Importance of quantum decoherence in brain processes. *Phys. Rev. E* 61: 4194–4206.

- [86] Schlosshauer M. 2007 *Decoherence and the Quantum to Classical Transition*. Springer, Berlin.
- [87] Zweir MC, Chong LT. 2010 Reaching biological timescales with all-atom molecular dynamics simulations. *Curr. Opin. Pharmacol.* 10: 745–752.
- [88] Marais A *et al.* 2018 The future of quantum biology. *J. R. Soc. Interface* 15: 20180640.
- [89] Cao J *et al.* 2020 Quantum biology revisited. *Science Adv.* 6: eaaz4888.
- [90] Kim, Y., Bertagna, F., D’Souza, E. M., Heyes, D. J., Johannissen, L. O., Nery, E. T. 2021 Quantum biology: an update and perspective. *Quant. Rep.* 3, 1–48.
- [91] Baiardi, A., Christandl, M., Reiher, M. 2022 Quantum computing for molecular biology. Preprint arXiv:2212.12220.
- [92] Fields, C.; Levin, M. 2021 Metabolic limits on classical information processing by biological cells. *BioSystems* 209, 104513.
- [93] Kerskens, C. M., Pérez, D. L. 2022 Experimental indications of non-classical brain functions. *J. Phys. Commun.* 6, 105001.
- [94] Fields, C.; Marcianò, A. 2019 Holographic screens are classical information channels. *Quant. Rep.* 2, 326–336.
- [95] Addazi, A.; Chen, P.; Fabrocini, F.; Fields, C.; Greco, E.; Lulli, M.; Marcianò, A.; Pasechnik, R. 2021 Generalized holographic principle, gauge invariance and the emergence of gravity à la Wilczek. *Front. Astron. Space Sci.* 8, 563450.
- [96] Fields, C.; Glazebrook, J. F.; Marcianò, A. 2022 The physical meaning of the holographic principle. *Quanta* 11, 72–96.
- [97] Pastawski, F.; Yoshida, B.; Harlow, D.; Preskill, J. 2015 Holographic quantum error-correcting codes: Toy models for the bulk/boundary correspondence. *J. High Energy Phys.* 6, 149.
- [98] Fields, C.; Glazebrook, J. F.; Marcianò, A. 2023 LOCC protocols and QECCs from the perspective of TQFT, in preparation.
- [99] Landauer, R. 1999 Information is a physical entity. *Physica A* 263, 63–67.
- [100] Bennett, C. H. 1982 The thermodynamics of computation. *Int. J. Theor. Phys.* 21, 905–940.
- [101] Seifert, U. 2012 Stochastic thermodynamics, fluctuation theorems and molecular machines. *Rep. Prog. Phys.* 75, 126001.
- [102] Atiyah, M. 1988 Topological quantum field theory. *Pub. Math. IHÉS* 68, 175–186.

- [103] Chitambar, E., Leung, D., Mančinska, L., Ozols, M., Winter, A. 2014 Everything you always wanted to know about LOCC (but were afraid to ask). *Comms. Math. Phys.* 328, 303–326.
- [104] Tipler, F. 2014 Quantum nonlocality does not exist. *Proc. Natl. Acad. Sci. USA* 111, 11281–11286.
- [105] Bell, J. S. 1966 On the problem of hidden variables in quantum mechanics. *Rev. Mod. Phys.* 38, 447–452.
- [106] Kochen, S., Specker, E. P. 1967 The problem of hidden variables in quantum mechanics. *J. Math. Mech.* 17, 59–87.
- [107] Mermin, N. D. 1993 Hidden variables and the two theorems of John Bell. *Rev. Mod. Phys.* 65, 803–815.
- [108] Qi, X.-L. 2018 Does gravity come from quantum information? *Nature Phys.* 14, 984–987, <https://doi.org/10.1038/s41567-018-0297-3>.
- [109] Bekenstein, J. D. Black holes and the second law. *Lett. Nuovo Cim.* 4, 737–740 (1972).
- [110] Bekenstein, J. D. Black holes and entropy. *Phys. Rev. D* 7, 2333–2346 (1973).
- [111] Hawking, S. W. Gravitational radiation from colliding black holes. *Phys. Rev. Lett.* 26, 1344–1346 (1971).
- [112] Hawking, S. W. Black hole explosions? *Nature* 248, 30–31 (1974).
- [113] Susskind, L. The world as a hologram. *J. Math. Phys.* 36, 6377–6396 (1995).
- [114] Bousso, R. The holographic principle. *Rev. Mod. Phys.* 74, 825–874 (2002).
- [115] 't Hooft, G. Dimensional reduction in quantum gravity. Preprint at <https://arxiv.org/abs/gr-qc/9310026> (1993).
- [116] Maldacena, J. The large-N limit of superconformal field theories and supergravity. *Int. J. Theor. Phys.* 38, 1113 (1999).
- [117] Almheiri, A., Dong, X. and Harlow, D. Bulk locality and quantum error correction in AdS/CFT. *J. High Energy Phys.* 2015, 163 (2015).
- [118] Hubeny, V. E. and Rangamani, M. Causal holographic information. *J. High Energy Phys.* 2012, 114 (2012).
- [119] Headrick, M., Hubeny, V. E., Lawrence, A. and Rangamani, M. Causality and holographic entanglement entropy. *J. High Energy Phys.* 2014, 162 (2014).
- [120] Swingle, B. Entanglement renormalization and holography. *Phys. Rev. D* 86, 065007 (2012).

- [121] White, S. R. Density matrix formulation for quantum renormalization groups. *Phys. Rev. Lett.* 69, 2863-2866 (1992).
- [122] Verstraete, F., Murg, V. and Cirac, J. I. Matrix product states, projected entangled pair states, and variational renormalization group methods for quantum spin systems. *Adv. Phys.* 57, 143-224 (2008).
- [123] DiVincenzo, D. P. et al. in *Quantum Computing and Quantum Communications* (ed. Williams, C. P.) 247-257 (Springer, Berlin, 1999).
- [124] Vidal, G. Class of quantum many-body states that can be efficiently simulated. *Phys. Rev. Lett.* 101, 110501 (2008).
- [125] Pastawski, F., Yoshida, B., Harlow, D. and Preskill, J. Holographic quantum error-correcting codes: toy models for the bulk/boundary correspondence. *J. High Energy Phys.* 2015, 149 (2015).
- [126] Yang, Z., Hayden, P. and Qi, X.-L. Bidirectional holographic codes and sub-AdS locality. *J. High Energy Phys.* 2016, 175 (2016).
- [127] Hayden, P. et al. Holographic duality from random tensor networks. *J. High Energy Phys.* 2016, 9 (2016).
- [128] Han, M. and Huang, S. Discrete gravity on random tensor network and holographic Rényi entropy. *J. High Energy Phys.* 2017, 148 (2017).
- [129] Lashkari, N., McDermott, M. B. and Van Raamsdonk, M. Gravitational dynamics from entanglement “thermodynamics”. *J. High Energy Phys.* 2014, 195 (2014).
- [130] Swingle, B. and Van Raamsdonk, M. Universality of gravity from entanglement. Preprint at <https://arxiv.org/abs/1405.2933> (2014).
- [131] Shenker, S. H. and Stanford, D. Black holes and the butterfly effect. *J. High Energy Phys.* 2014, 67 (2014).
- [132] Sachdev, S. and Ye, J. Gapless spin-fluid ground state in a random quantum Heisenberg magnet. *Phys. Rev. Lett.* 70, 3339-3342 (1993).
- [133] Kitaev, A. A simple model of quantum holography. KITP <http://online.kitp.ucsb.edu/online/entangled15/kitaev/>; <http://online.kitp.ucsb.edu/online/entangled15/kitaev2/> (2015).
- [134] Maldacena, J. and Stanford, D. Remarks on the Sachdev-Ye-Kitaev model. *Phys. Rev. D* 94, 106002 (2016).
- [135] Smith, J. E., Nair, R. 2005 The architecture of virtual machines. *IEEE Computer* 38(5), 32–38.

- [136] Manevitz, L. M., Yousef, M. 2002 One-class SVMs for document classification. *J. Mach. Learn. Res.* 2, 139–154.
- [137] Kosko, B. 1988 Bidirectional associative memories. *IEEE Trans. Syst. Man Cybern.* 18, 49–60.
- [138] J. Baez, Lett. Math. Phys. 1996, 38, 129.
- [139] Rovelli, C. Quantum Gravity, Cambridge University Press, Cambridge, UK 2004.
- [140] Fields, C. Glazebrook, F. and Marcianò, A. Sequential Measurements, Topological Quantum Field Theories, and Topological Quantum Neural Networks, *Fortschr. Phys.* 2022, 2200104.
- [141] Parisi, G. and Wu, Y.-S. Perturbation theory without gauge fixing, *Scientia Sinica* 24, 483 (1981); doi: 10.1360/ya1981-24-4-483, <http://engine.scichina.com/doi/10.1360/ya1981-24-4-483>.
- [142] Lulli, M., Marcianò, A. and Shan, X. Stochastic Quantization of General Relativity à la Ricci-Flow, [arXiv:2112.01490 [gr-qc]].
- [143] Marcianò, A. *in preparation*.
- [144] Sengupta, R. Adhikary, S. Oseledets, I. and Biamonte, J. Tensor Networks in Machine Learning, <https://arxiv.org/pdf/2207.02851.pdf>, 2022.
- [145] E. Miles Stoudenmire, Talk at the International Center for Theoretical Physics Trieste, August 2018.
- [146] Stoudenmire, E.M. Schwab, D.J. Supervised Learning with Quantum-Inspired Tensor Networks, <https://arxiv.org/abs/1605.05775>, 2016.
- [147] Novikof, A. Trofimov, M. and Oseledets, I. Exponential Machines, <https://arxiv.org/abs/1605.03795>, 2017.
- [148] Glasser, I. Pancotti, N. and Cirac, J.I. From probabilistic graphical models to generalized tensor networks for supervised learning, <https://arxiv.org/abs/1806.05964>, 2018.
- [149] Han, Z.-H. Wang, J. Fan, H. Wang, L. and Zhang, P. Unsupervised Generative Modeling Using Matrix Product States, in *Physical Review X*, 8, 2018.
- [150] Liu, J. Li, S.-J. Zhang, J. and Zhang, P. Tensor networks for unsupervised machine learning, <https://arxiv.org/abs/2106.12974>, 2021.
- [151] Convy, I. and Whaley, K.B. Interaction Decompositions for Tensor Network Regression, <https://arxiv.org/abs/2208.06029>, 2022.

- [152] Groenhof, G. 2013 Introduction to QM/MM simulations. *Methods Mol. Biol.* 924, 43–66.
- [153] Ledezma-Tejeida, D.; Schastnaya, E.; Sauer, U. 2021 Metabolism as a signal generator in bacteria. *Curr. Opin. Syst. Biol.* 28, 100404.
- [154] Fields, C.; Friston, K.; Glazebrook, J. F.; Levin, M.; Marcianò, A. 2022 The free energy principle induces neuromorphic development. *Neuromorph. Comp. Engin.* 2, 042002.
- [155] Fields, C.; Glazebrook, J. F.; Levin, M. 2022 Neurons as hierarchies of quantum reference frames. *Biosystems* 219, 104714.
- [156] Fields, C., Levin, M. 2022 Competency in navigating arbitrary spaces as an invariant for analyzing cognition in diverse embodiments. *Entropy* 24, 819.
- [157] Bain, J. 2020 Spacetime as a quantum error-correcting code? *Stud. Hist. Phil. Mod. Phys.* 71, 26–36.
- [158] Flombaum, J. I.; Scholl, B. J.; Santos, L. R. 2008 Spatiotemporal priority as a fundamental principle of object persistence. In: *The Origins of Object Knowledge*, eds B. Hood and L. Santos (Oxford: Oxford University Press), 135–164.
- [159] Fields, C. 2011 Trajectory recognition as the basis for object individuation: A functional model of object file instantiation and object-token encoding. *Front. Psychol.* 2, 49.
- [160] Niss, K.; Gomez-Casado, C.; Hjaltelin, J. X.; Joeris, T.; Agace, W. W.; Belling, K. G.; Brunak, S. 2020 Complete topological mapping of a cellular protein interactome reveals bow-tie motifs as ubiquitous connectors of protein complexes. *Cell Rep.* 31, 107763.
- [161] Carafoli, E. and Krebs, J. Why calcium? How calcium became the best communicator. *J. Biol Chem* 40 2016, 20849–20857.
- [162] Polouliakh, N., Nock, R., Nielsen, F. and Kitano, H. G-protein coupled receptor signaling architecture of mammalian immune cells. *PLoS ONE* 4(1) 2009, e4189.
- [163] Friedlander, T., Mayo, A. E., Tlusty, T. and Alon, U. Evolution of bow-tie architectures in biology. *PLOS Computational Biology* 11(3) 2015, e1004055
- [164] Boniolo, G., D'Agostino, M., Piazza, M. and Pulcini, G. Molecular biology meets logic: Context-sensitivity in focus. *Foundations of Science* 2021 in press, <https://doi.org/10.1007/s10699-021-09789-y>
- [165] Kingma, D. P and Welling, M. An Introduction to variational autoencoders. *Foundations and Trends in Machine Learning* 12(4) (2019), 307–392.

- [166] Dean, S. N. and Walper, S. A. Variational autoencoder for generation of antimicrobial peptides. *ACS Omega* 5 2020, 20746–20754.
- [167] Cervantes, V. H., Dzhafarov, E. N. (2018). Snow Queen is evil and beautiful: Experimental evidence for probabilistic contextuality in human choices. *Decision* 5(3), 193–204.
- [168] Wang, D., Sadrzadeh, Abramsky, S. and Cervantes, V. H. On the quantum-like contextuality of ambiguous phrases. *Proceedings of the 2021 Workshop on Semantic Spaces at the Intersection of NLP, Physics and Cognitive Science*, pp. 42–52. Association for Computational Linguistics 2021.
- [169] Editorial Focus. 2019 A matter of context. *Nature Immunol.* 20, 769.
- [170] Atlan, H. and Cohen, I. R. 1998 Immune information, self-organization and meaning. *Int. Immunology* 10, 711–717.
- [171] Basieva I, Khrennikov A, Ohya M, Yamato O. Quantum-like interference effect in gene expression: glucose-lactose destructive interference. *Syst Synth Biol* 2011;5:59–68.
- [172] Khrennikov, A. Quantum-like modeling of cognition. *Front Phys* 3 2015:77.
- [173] Barrett, L. F., and Simmons, W. K. (2015) Interoceptive predictions in the brain. *Nat. Rev. Neurosci.* **16**(7): 419–429.
- [174] Barrett, L. F. The theory of constructed emotion: an active inference account of interoception and categorization. *Soc. Cogn. Affect. Neurosci.* 12 2017, 1–23.
- [175] Conant RC, Ashby WR. Every good regulator of a system must be a model of that system. *Int. J. Syst. Sci.* 1970;1(2):89–97.
- [176] Hohwy, J. *The Predictive Mind*. Oxford University Press, Oxford, UK, 2013
- [177] Kleckner, I. R. et al. Evidence for a large-scale brain system supporting allostasis and interoception in humans. *Nature Human Behaviour* 11 2017, Article 0069, 14 pages.
- [178] Seth, A. K., Suzuki, K, and Critchley, H. D. An interoceptive predictive coding model of conscious presence. *Frontiers in Psychology* 2 Article 395, 16 pages.
- [179] Seth, A. K. (2013) Interoceptive inference, emotion, and the embodied self. *Trends in Cognitive Science* **17** (11): 565–573.
- [180] Pezzulo, G., Levin, M. 2016 Top-down models in biology: explanation and control of complex living systems above the molecular level. *J. R. Soc. Interface* 13(124), 20160555.
- [181] Birnbaum, K. D., Sánchez Alvarado, A. 2008 Slicing across kingdoms: Regeneration in plants and animals. *Cell* 132(4), 697–710.

- [182] Levin, M. 2022 Collective intelligence of morphogenesis as a teleonomic process. Preprint PsyArXiv hqc9b.
- [183] Biswas, S., Clawson, W., Levin, M. 2023 Learning in transcriptional network models: Computational discovery of pathway-level memory and effective interventions. *int. J. Molec. Sci.* 24(1), 285.
- [184] Emmons-Bell, M., Durant, F., Tung, A. et al. 2019 Regenerative adaptation to electrochemical perturbation in planaria: A molecular analysis of physiological plasticity. *iScience* 22, 147–165.
- [185] Clawson, W., Levin, M. 2022 Endless forms most beautiful 2.0: Teleonomy and the bioengineering of chimaeric and synthetic organisms. *Biol. J. Linnean Soc.* 2022, blac073.